16th European Research Conference on Electromagnetic Interactions with Nucleons and Nuclei

Pre Conference Workshops: 26 & 27 October 2025

Conference: 27 October - 1 November 2025

Constraining the GPD E: Deeply Virtual Compton Scattering off the neutron with CLAS12 at Jefferson Lab

> M. A. HOBALLAH on behalf of the CLAS Collaboration













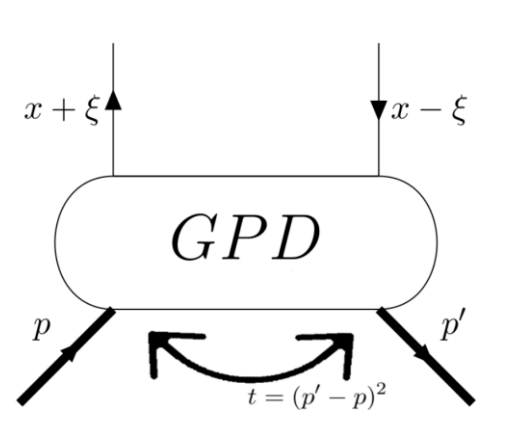
Generalized Parton Distributions - GPDs

Belitsky, Radyushkin, Physics Reports, 2005

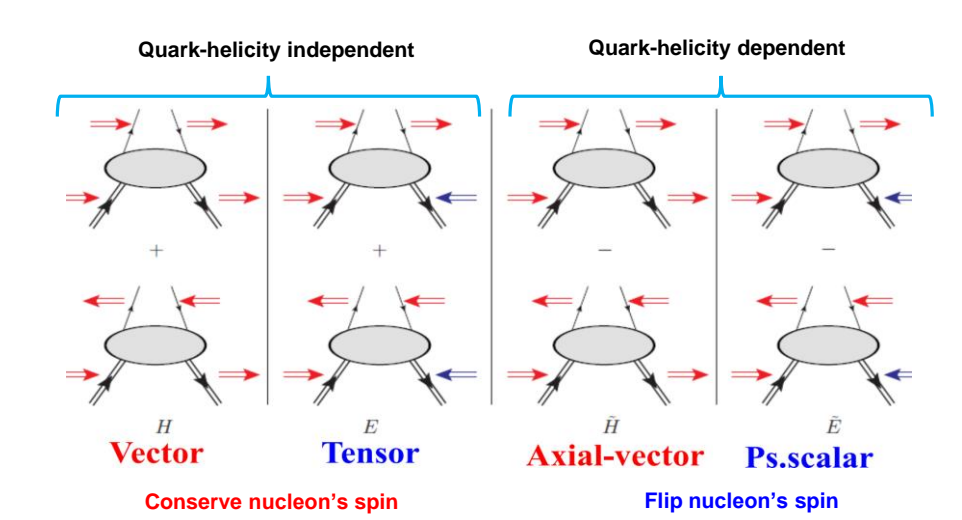
- Nucleon structure studies: QCD at low energies, a non-perturbative regime
 - Need structure functions to describe the nucleon

GPDs quantify correlations of transverse position and longitudinal momentum of partons in a hadron

- For the nucleon, there are 8 GPDs at leading-twist that describe the various combinations between nucleon/quark helicity states
- At leading order QCD, chiral-even (quark helicity is conserved), quark sector: 4 GPDs for each quark flavor H, \widetilde{H}, E and \widetilde{E}
- GPDs can be accessed through exclusive leptoproduction reactions
- GPDs depend on x, ξ and t = $(p' p)^2$



		Quark Polarization		
		Unpolarized (U)	Longitudinally Polarized (L)	Transversely Polarized (T)
Nucleon Polarization	U	Н		$2\widetilde{H}_T + E_T$
	L		\widetilde{H}	\widetilde{E}_T
	т	Е	\widetilde{E}	$H_{\scriptscriptstyle T}, \widetilde{H}_{\scriptscriptstyle T}$



M. A. HOBALLAH EINN 2025



Properties of GPDs and Why they are important?

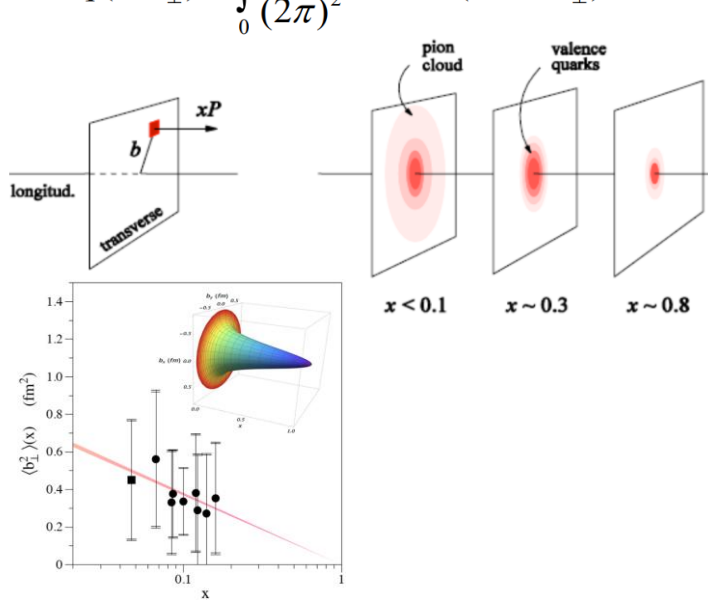
- GPDs are well-constrained functions: Fourier transforms of non-local, non-diagonal QCD operators
- They are universal: The same GPDs parametrize different processes: DVCS, DVMP, DDVCS, TCS (PRL 127, 262501, 2021)

Nucleon tomography

M. Burkardt, PRD 62, 71503 (2000)

$$q(x, \mathbf{b}_{\perp}) = \int_{0}^{\infty} \frac{d^{2} \Delta_{\perp}}{(2\pi)^{2}} e^{i\Delta_{\perp} \mathbf{b}_{\perp}} H(x, 0, -\Delta_{\perp}^{2})$$
$$\Delta q(x, \mathbf{b}_{\perp}) = \int_{0}^{\infty} \frac{d^{2} \Delta_{\perp}}{(2\pi)^{2}} e^{i\Delta_{\perp} \mathbf{b}_{\perp}} \widetilde{H}(x, 0, -\Delta_{\perp}^{2})$$

$$\Delta q(x, \mathbf{b}_{\perp}) = \int_{0}^{\infty} \frac{d^{2} \Delta_{\perp}}{(2\pi)^{2}} e^{i\Delta_{\perp} \mathbf{b}_{\perp}} \widetilde{H}(x, 0, -\Delta_{\perp}^{2})$$



R. Dupré, M. Guidal, M. Vanderhaeghen, PRD95, 011501 (2017)

Quark angular momentum

X. Ji, Phy.Rev.Lett.78,610(1997)

$$\frac{1}{2} \int_{-1}^{1} x dx (H(x, \xi, t = 0) + E(x, \xi, t = 0)) = J = \frac{1}{2} \Delta \Sigma + \Delta L$$

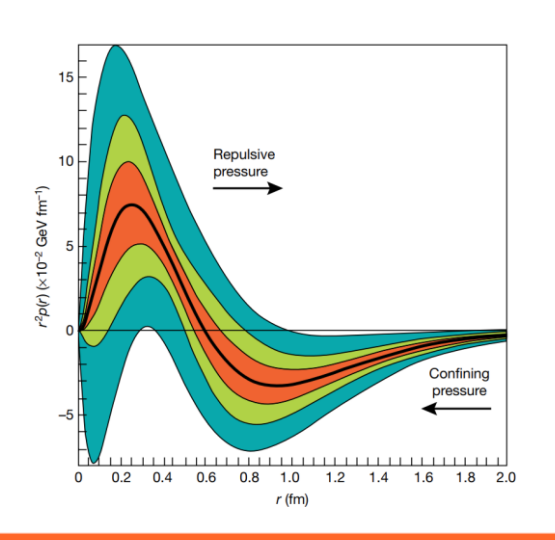
Nucleon spin: $\frac{1}{2} = \frac{1}{2}\Delta\Sigma + \Delta L + \Delta G$

- The intrinsic spin of the quarks can not explain the origin of the spin of the nucleon (nucleon **Spin Crisis)**
- Intrinsic spin of the gluons
- GPDs: quantify the contribution of orbital angular momentum of quarks to the nucleon spin

The pressure distribution inside proton

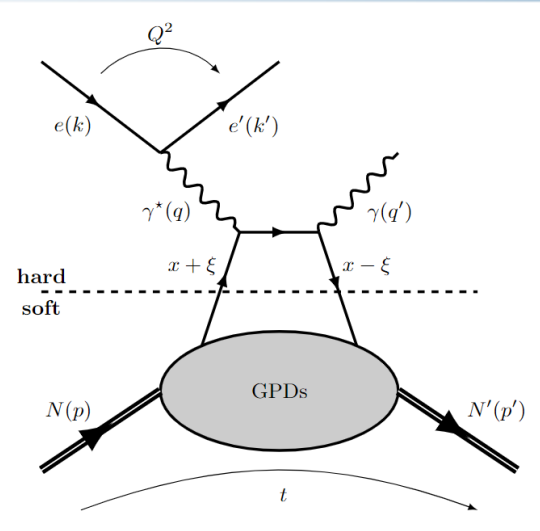
V. Burkert, L. Elouadrhiri, F.X. Girod, Nature 557, 396-399 (2018)

- Gravitational form factor
 - $\int xH(x,\xi,t)dx = M_2(t) + \frac{4}{5}\xi^2 d_1(t)$
 - $d_1(t) \propto \int \frac{j_0(r\sqrt{-t})}{2t} \rho(r) d^3r$





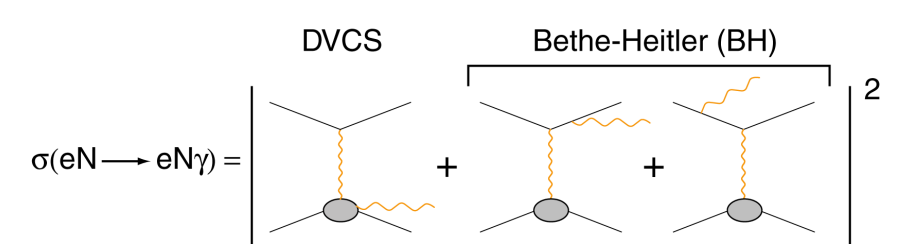
Deeply Virtual Compton Scattering of leptons off nucleons



- DVCS allows access to 4 complex GPDs-related quantities (only helicity-conserved terms are considered):
 - Compton Form Factors (x, ξ,t) (CFFs)

$$\mathcal{H} = \sum_{q} e_{q}^{2} \left\{ i \, \pi \left[H^{q}(\xi, \xi, t) - H^{q}(-\xi, \xi, t) \right] \, + \, \mathcal{P} \int_{-1}^{1} dx H^{q}(x, \xi, t) \left[rac{1}{\xi - x} - rac{1}{\xi + x}
ight] \,
ight\}$$

x cannot be accessed experimentally by DVCS:
 Models needed to map the x dependence



BH is purely electromagnetic and parametrised by FFs

- The DVCS-BH interference term (linear in CFFs)
 - Access the phase of the DVCS amplitude: isolate imaginary and real parts of CFFs.
- Experimentally measured observables: Access to a combinations of CFFs
- > Separation of CFFs: measurement of several observables
- Proton or Neutron: different sensitivity to the CFFs (GPDs)
- > Flavor separation of GPDs: need measurements on both nucleons

$$(H,E)_{u}(\xi,\xi,t) = \frac{9}{15} \Big[4(H,E)_{p}(\xi,\xi,t) - (H,E)_{n}(\xi,\xi,t) \Big]$$

$$(H,E)_{d}(\xi,\xi,t) = \frac{9}{15} \Big[4(H,E)_{n}(\xi,\xi,t) - (H,E)_{p}(\xi,\xi,t) \Big]$$



Deeply Virtual Compton Scattering: physics observables and their link to CFFs

Belitsky, Müller, Kirner, Nuc. Phys. B 629 (2002)

Polarized beam, unpolarized taget

$$\Delta \sigma_{LU} \sim \sin(\phi) \Im \{F_1 \mathbf{H} + \xi (F_1 + F_2) \widetilde{\mathbf{H}} - k F_2 \mathbf{E} + \dots \}$$

Unpolarized beam, polarized target

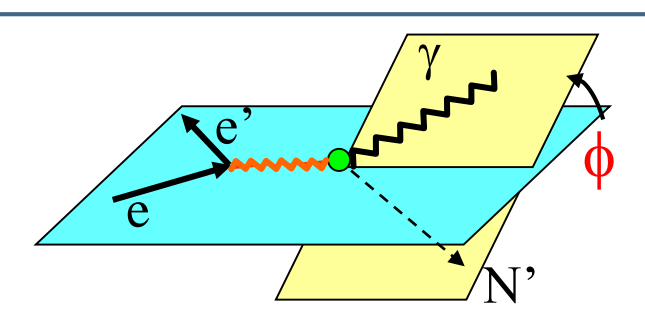
$$\Delta \sigma_{UL} \sim \sin(\phi) \Im \left\{ F_1 \widetilde{\boldsymbol{H}} + \xi (F_1 + F_2) \left(\boldsymbol{H} + \frac{x_b}{2} \boldsymbol{E} \right) - \xi k F_2 \widetilde{\boldsymbol{E}} \right\}$$

polarized beam, longitudinal polarized target

$$\Delta \sigma_{LL} \sim (A + B \cos(\phi)) \Re \{F_1 \widetilde{\mathbf{H}} + \xi (F_1 + F_2) \left(\mathbf{H} + \frac{x_b}{2} \mathbf{E} \right) + \dots \}$$

unpolarized beam, transverse polarized target

$$\Delta \sigma_{UT} \sim \cos(\phi) \sin(\phi_s - \phi) \Im\{k(F_2 \mathbf{H} - F_1 \mathbf{E}) + ...\}$$



Different contributions from F_1 and F_2 for the different nucleons

Observable	Proton	Neutron
$\Delta\sigma_{LU}$	$\Im\{\boldsymbol{H_p},\widetilde{H}_p,E_p\}$	$\Im\{H_n,\widetilde{H}_n,\pmb{E_n}\}$
$\Delta\sigma_{UL}$	$\Im\{H_p,\widetilde{H}_p\}$	$\Im\{\boldsymbol{H_n}, E_n\}$
$\Delta\sigma_{LL}$	$\Re\{H_p,\widetilde{H}_p\}$	$\Re\{\boldsymbol{H_n}, E_n\}$
$\Delta\sigma_{UT}$	$\Im\{H_p, E_p\}$	$\Im\{H_n\}$

e.g. (in experiment):

$$\Delta \sigma_{LU} = \frac{1}{Pol_{\bullet}} \times \frac{N^{+} - N^{-}}{N^{+} + N^{-}}$$

Computed as a function of the angle ϕ



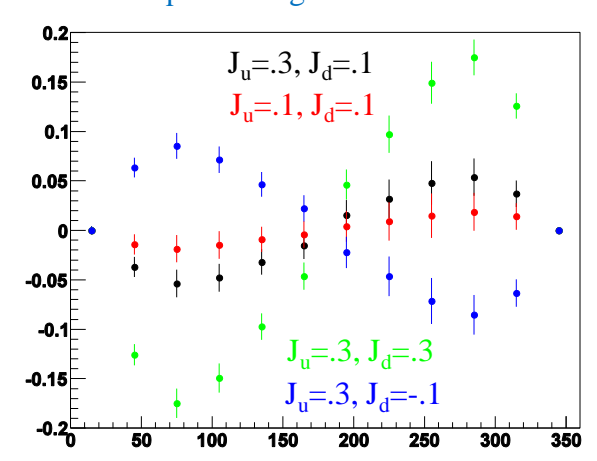
The GPD E: a missing piece in the puzzle

- GPD E, one of the least constrained GPD
- DVCS with an unpolarized deuterium target :
- Scattering off neutron (nDVCS): GPD E
 - The unpolarized cross section is sensitive mainly to the real part of CFF E
 - Beam Spin Asymmetry (and the polarized cross-section difference) is sensitive to the imaginary part of CFF E
 - Determination of Ji sum rule
- To get a clear understanding of the GPD E: the BSA for nDVCS is
 - Complementary to the TTSA for pDVCS on transverse target, aiming at E
 - Depends strongly on the kinematics → wide coverage needed
 - Smaller than for pDVCS → more beam time needed to achieve reasonable statistics

Different contributions from F_1 and F_2 for the different nucleons

Observable	Proton	Neutron
$\Delta\sigma_{LU}$	$\Im\{\pmb{H_p},\widetilde{H}_p,E_p\}$	$\Im\{H_n,\widetilde{H}_n,m{E_n}\}$
$\Delta\sigma_{UL}$	$\Im\{H_p,\widetilde{H}_p\}$	$\Im\{\boldsymbol{H_n}, E_n\}$
$\Delta\sigma_{LL}$	$\Re\{\pmb{H_p}, \widetilde{\pmb{H}_p}\}$	$\Re\{\boldsymbol{H_n}, E_n\}$
$\Delta\sigma_{UT}$	$\Im\{H_p,E_p\}$	$\Im\{H_n\}$

Model predictions (VGG) for different values of quarks' angular momentum

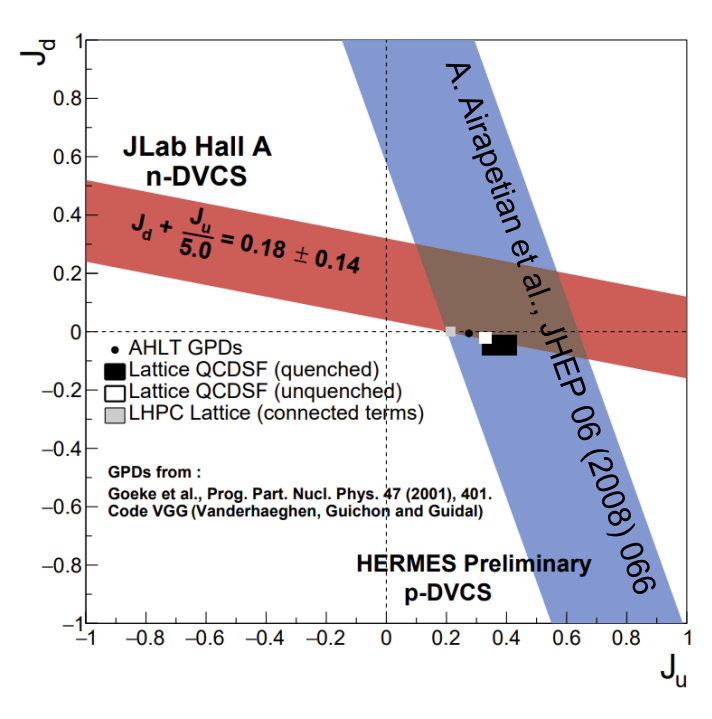


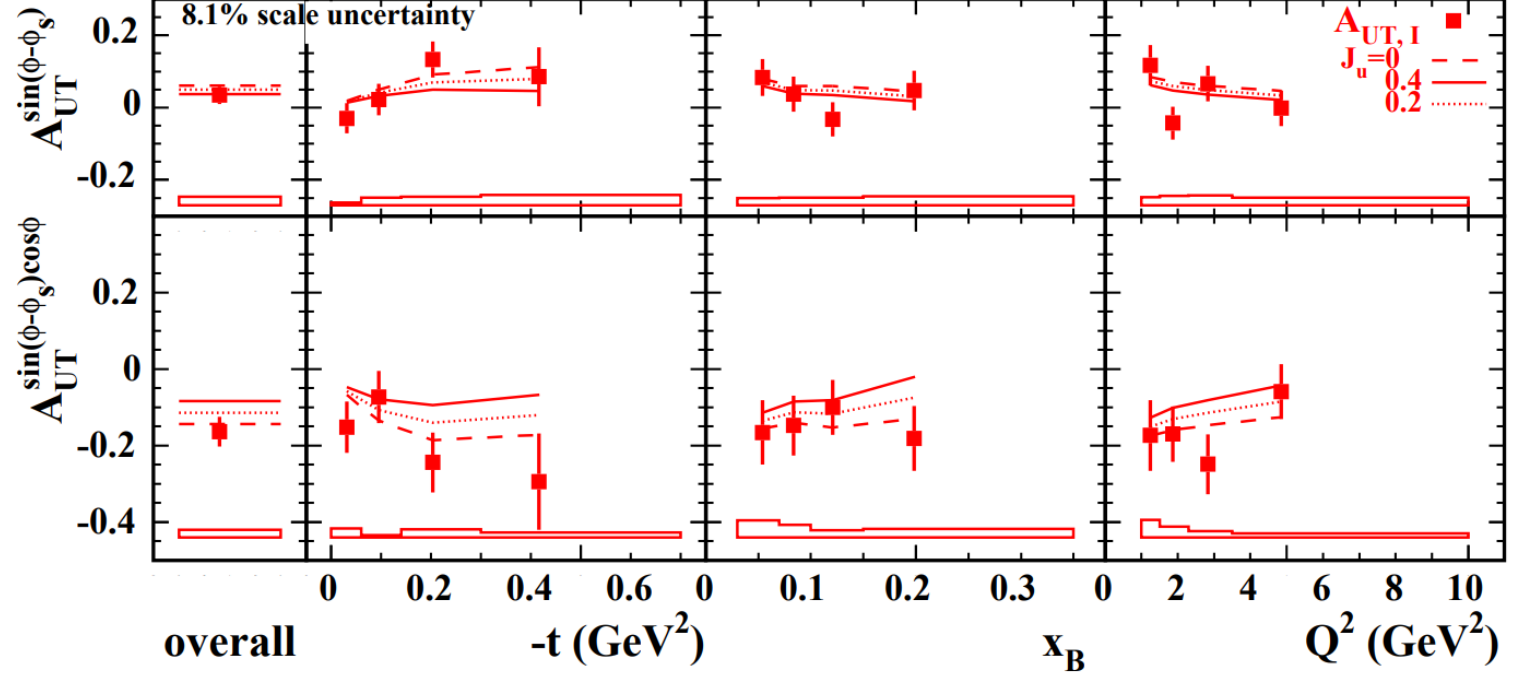


The GPD E: previous experiments

- HERMES measured DVCS off a transversely polarized proton target
- A. Airapetian et al., JHEP 06 (2008) 066
- Observables sensitive to the GPD E: Transverse Target Spin Asymmetry

Unpolarized beam, Transverse polarized target $\Delta \sigma_{UT} \sim \cos(\phi) \sin(\phi_s - \phi) \Im\{k(F_2 \mathbf{H} - F_1 \mathbf{E}) + ...\}$



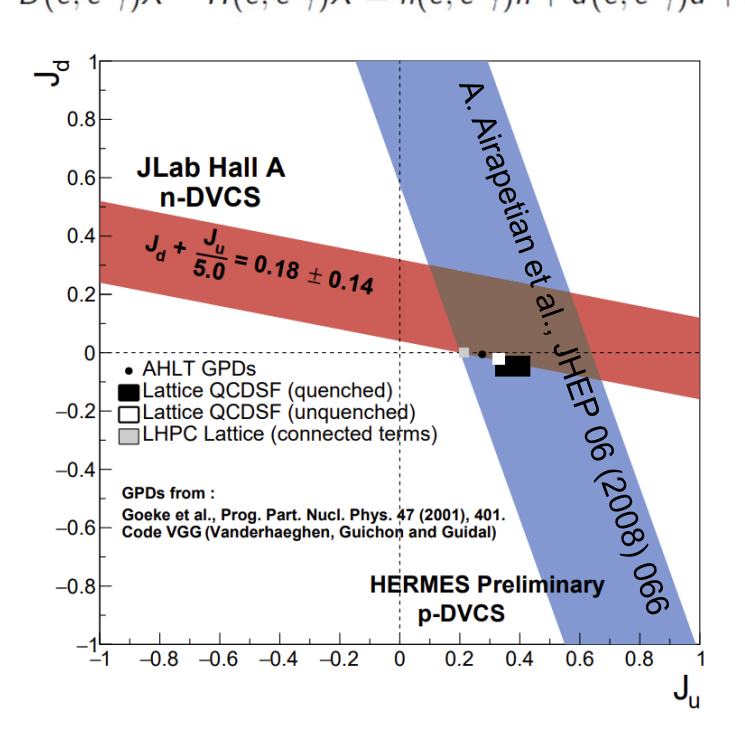


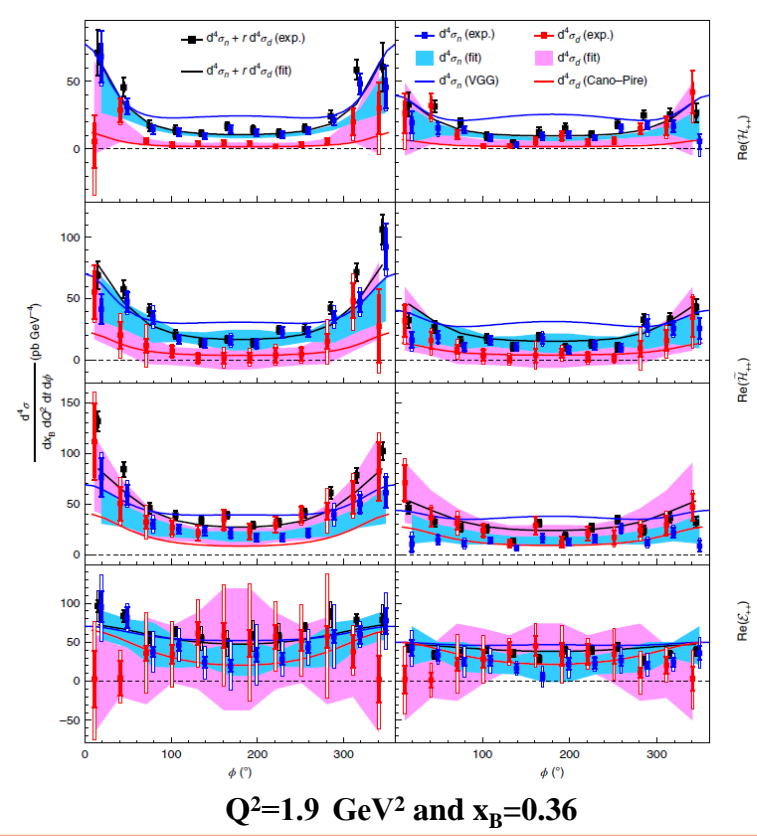


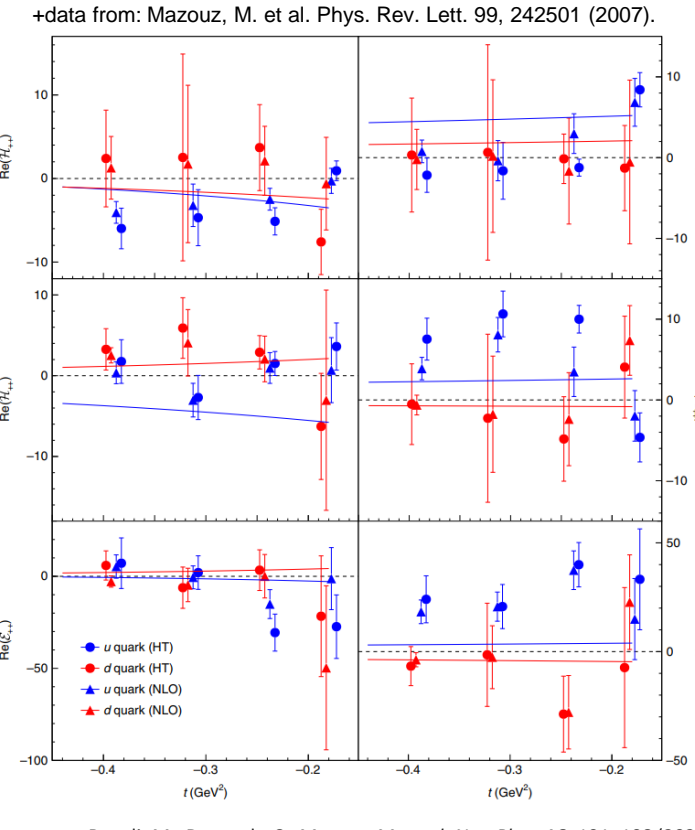
The GPD E: previous experiments

- Previous pioneering measurement of nDVCS (Jlab Hall A @ 6 GeV)
 - Beam-energy « Rosenbluth » separation of nDVCS CS using an LD2 target and two different beam energies
 - First observation of non-zero nDVCS CS
- No neutron detection

$$D(e, e'\gamma)X - H(e, e'\gamma)X = n(e, e'\gamma)n + d(e, e'\gamma)d + \dots$$





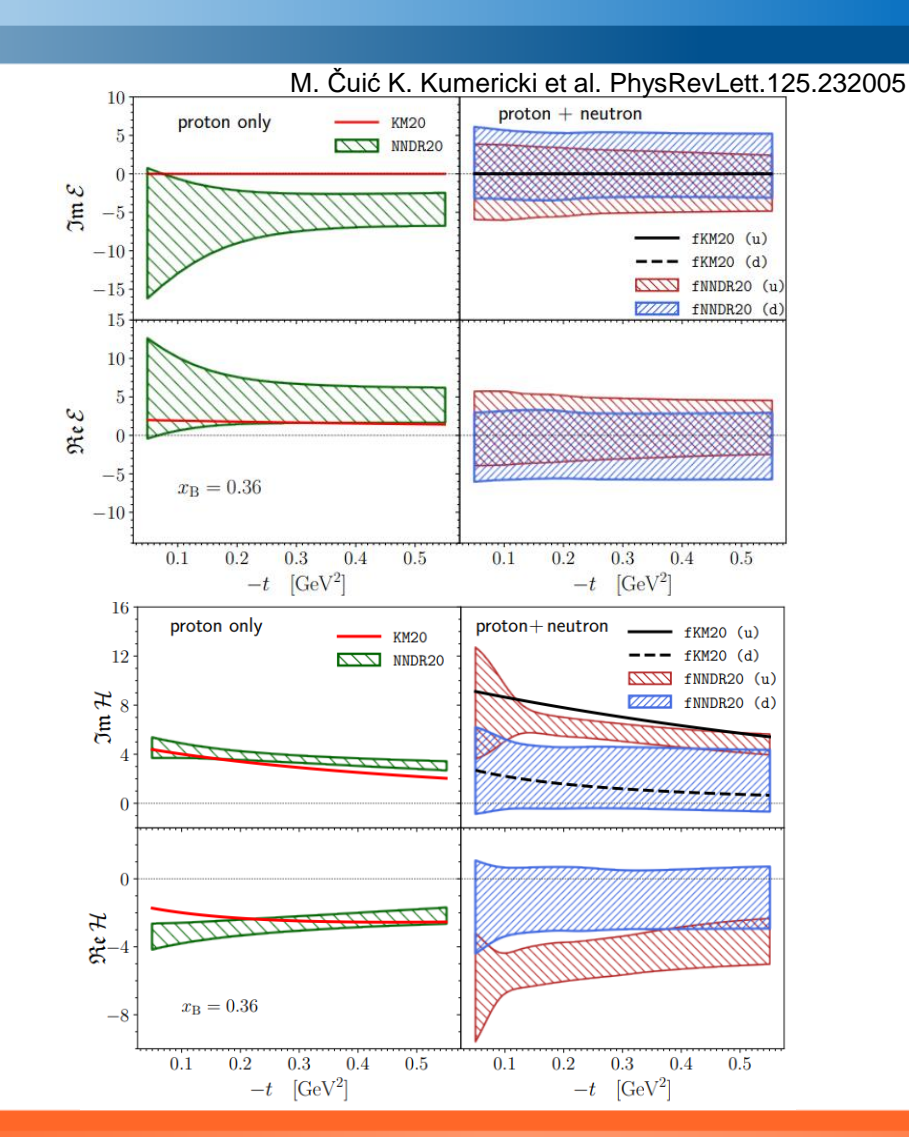


Benali, M., Desnault, C., Mazouz, M. et al. Nat. Phys. 16, 191-198 (2020)



The GPD E: previous experiments

- Use of Neural Networks (NN) to perform a model-independent CFF evaluations
- Input are measurements of spin-dependent observables and cross section values
 - Proton and neutron data from Jlab (clas6 and Hall A)
- The presence of CLAS6 neutron data allows a flavor separation
 - Up and down contributions to CFF H separated
 - CFF E flavors are not separated, a significant sign ambiguity remains





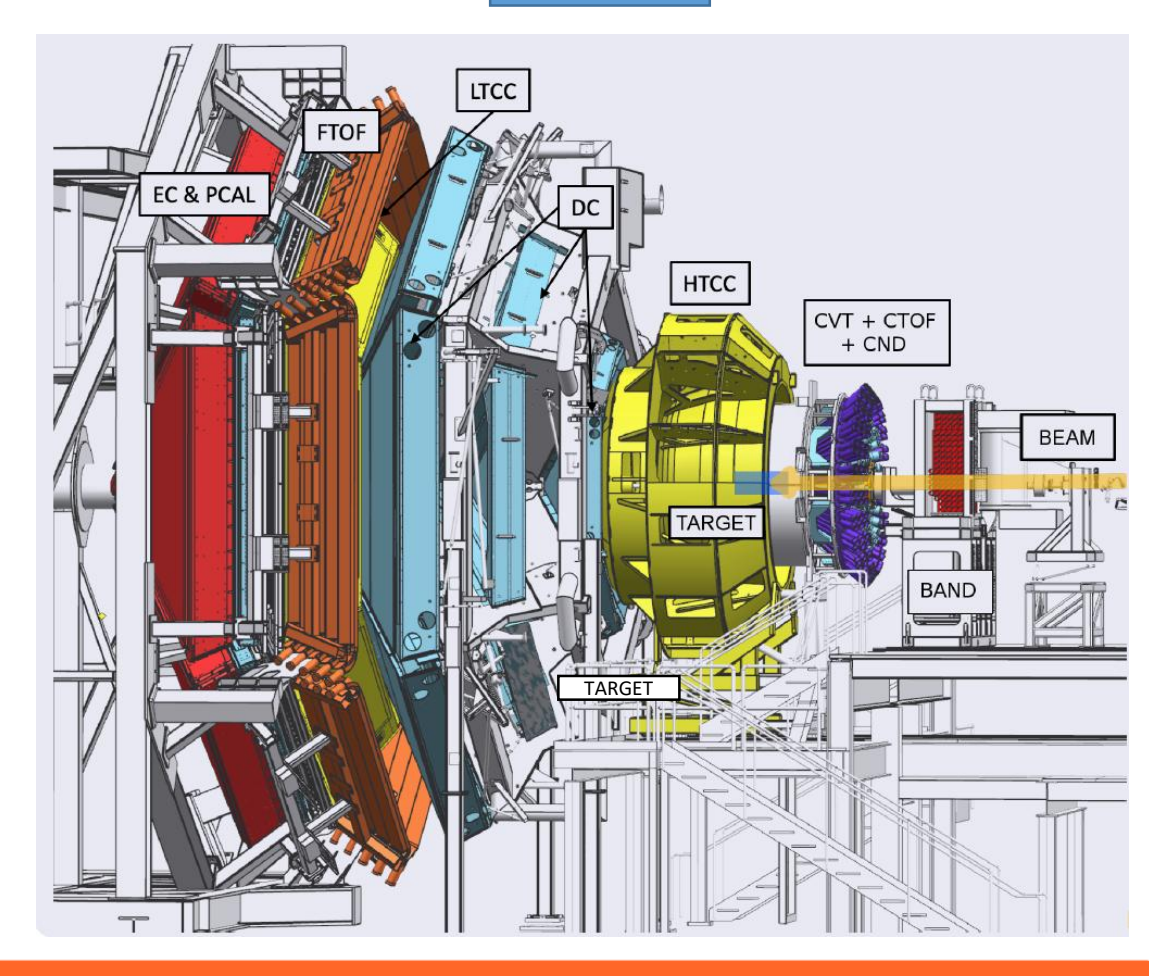
The CEBAF and CLAS at Jefferson Laboratory

Continuos Electron Beam Accelerator Facility

- Up to 12 GeV electrons
- Two anti-parallel linacs, with recirculating arcs on both ends
- 4 experimental halls



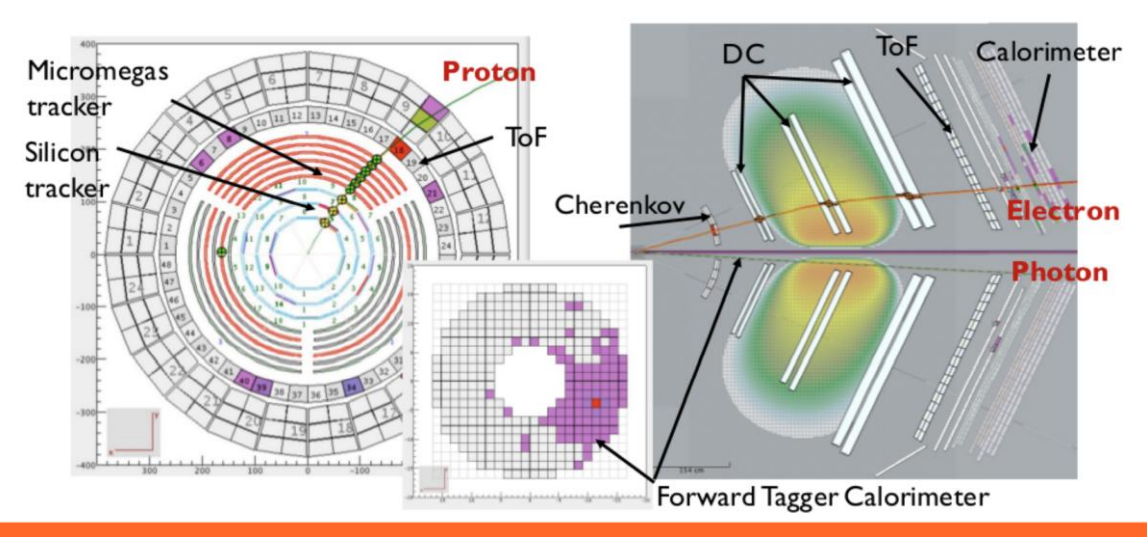
CLAS12





CLAS12: DVCS with an unpolarized deuterium target

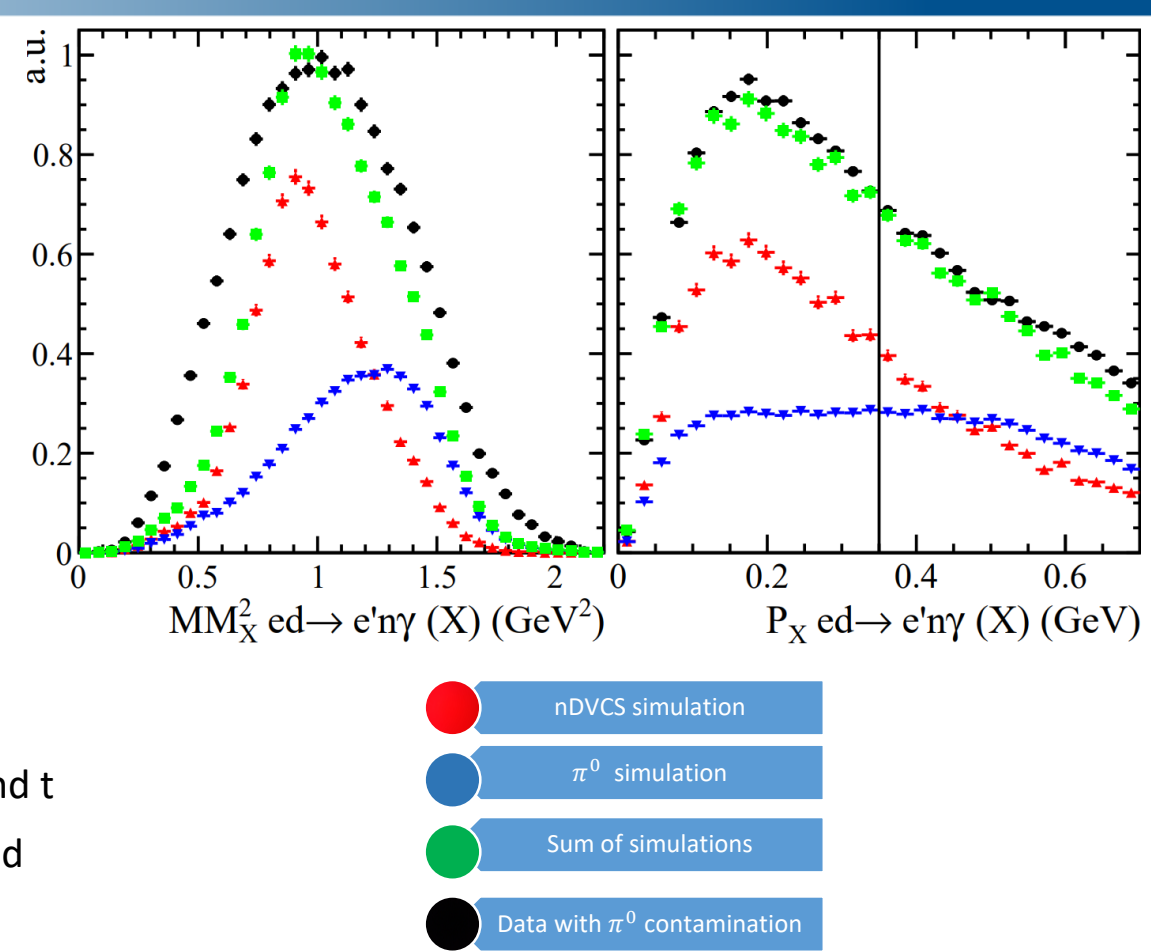
- A 10.6/10.4/10.2 GeV electron beam
 - With an average polarization of 86%
 - Scattering off an unpolarized Liquid Deuterium target of 5 cm length
- The exclusivity of the event is insured by:
 - Electron detection: Cerenkov detector, drift chambers and electromagnetic calorimeter
 - Photon detection: sampling calorimeter or a small PbWO4-calorimeter close to the beamline
 - Proton detection: Silicon and Micromegas detector OR Neutron detection: Central Neutron Detector
- For Neutron Detection:
 - Machine Learning techniques are applied to improve the Identification and reduce charged particle contamination





CLAS12: DVCS with an unpolarized deuterium target

- The nDVCS (pDVCS) final state is selected with the following exclusivity criteria: (N:nucleon)
 - Missing mass
 - $ed \rightarrow eN\gamma X$
 - $e N \rightarrow e N \gamma X$
 - $e N \rightarrow e N X$
 - Missing momentum
 - $ed \rightarrow eN\gamma X$
 - ΔΦ, Δt, θ(γ,X)
 - Difference between two ways of calculating Φ and t
 - Cone angle between measured and reconstructed photon



 π^0 background contamination is estimated using simulations



π^0 background subtraction

- Subtraction using simulations of the background channel
 - Monte Carlo simulations:
 - GPD-based event generator for DVCS/pi0 on deuterium
 - DVCS amplitude calculated according to the BKM formalism
 - Fermi-motion distribution evaluated according to Paris potential
- 1. Estimate the ratio of partially reconstructed eN $\pi^0(1 \text{ photon})$ decay to fully reconstructed eN π^0 decays in MC
- 2. This is done for each kinematic bin to minimize MC model dependence
- 3. Multiply this ratio by the number of reconstructed eN π^0 in data to get the number of eN $\pi^0(1$ photon) in data
- 4. Subtract this number from DVCS reconstructed decays in data per each kinematical bin

Simulations:
$$R = \frac{N(eN\pi_{1\gamma}^0)}{N(eN\pi^0)}$$

Data: $N(eN\pi_{1\gamma}^0) = R * N(eN\pi^0)$
 $N(DVCS) = N(DVCS_{recon}) - N(eN\pi_{1\gamma}^0)$

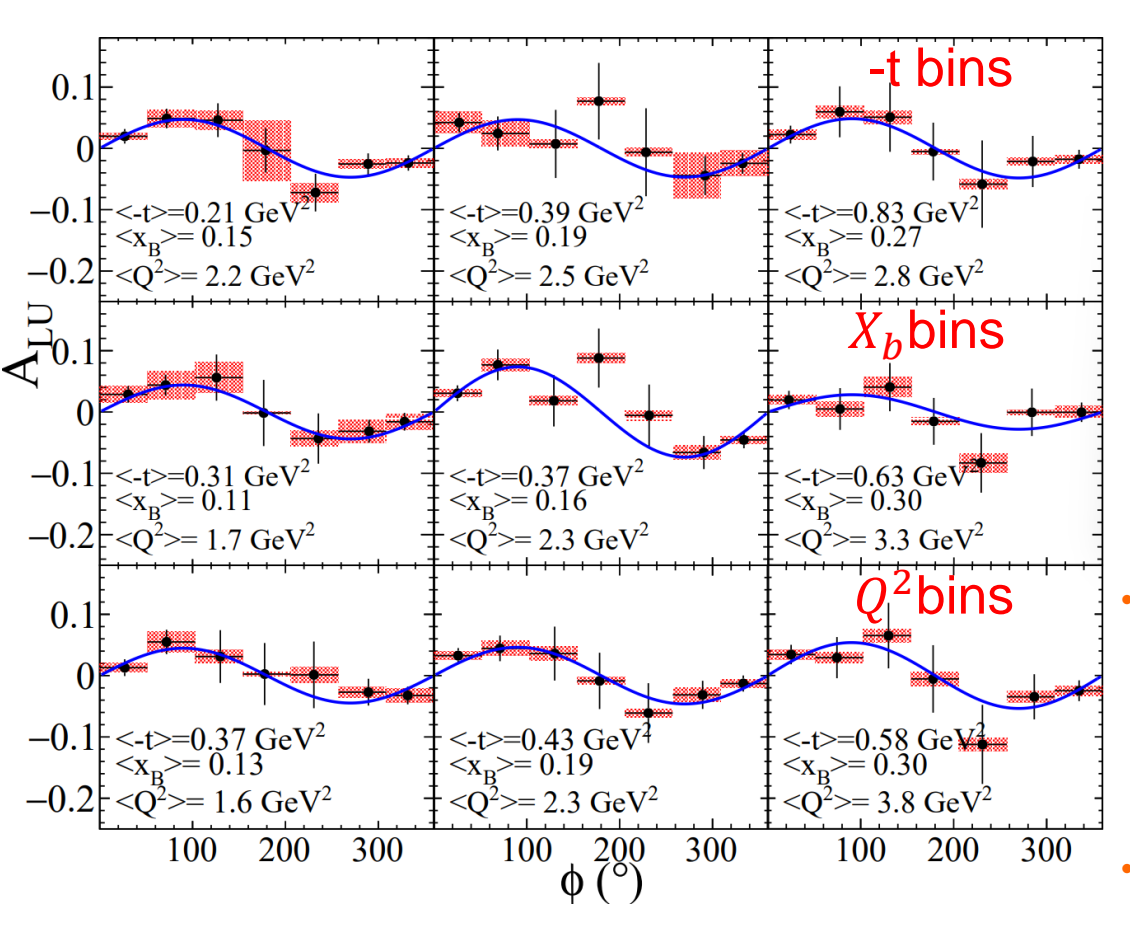
 π^0 background subtraction is also performed by statistical unfolding of contribution to the missing mass spectrum M. Pivk and F.R. Le Diberder, NIMA 555 1 2005 Signal from simulations Background from simulation nDVCS data

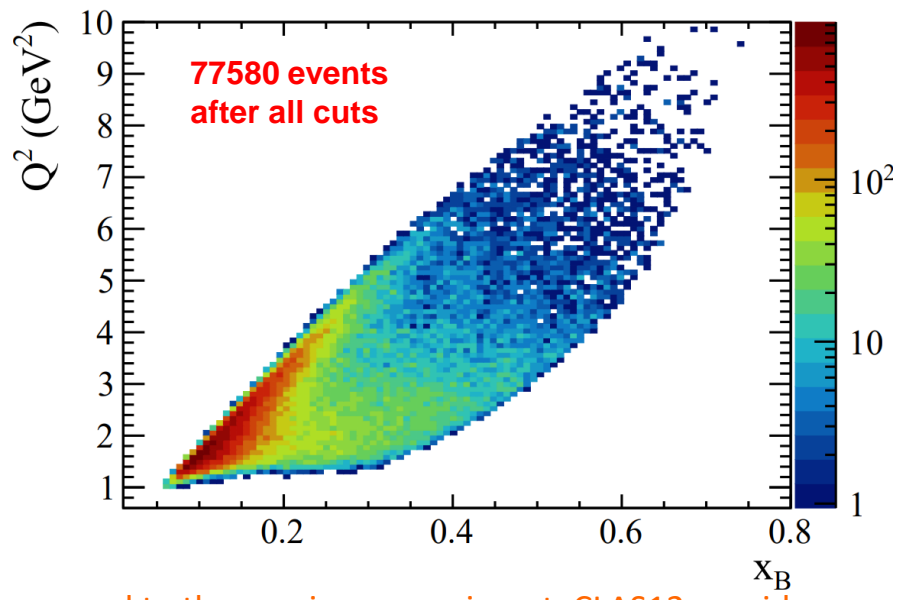
The difference between the estimations of background from both methods is considered as a systematic



CLAS12: nDVCS with an unpolarized deuterium target

First-time measurement of nDVCS with detection of the active neutron



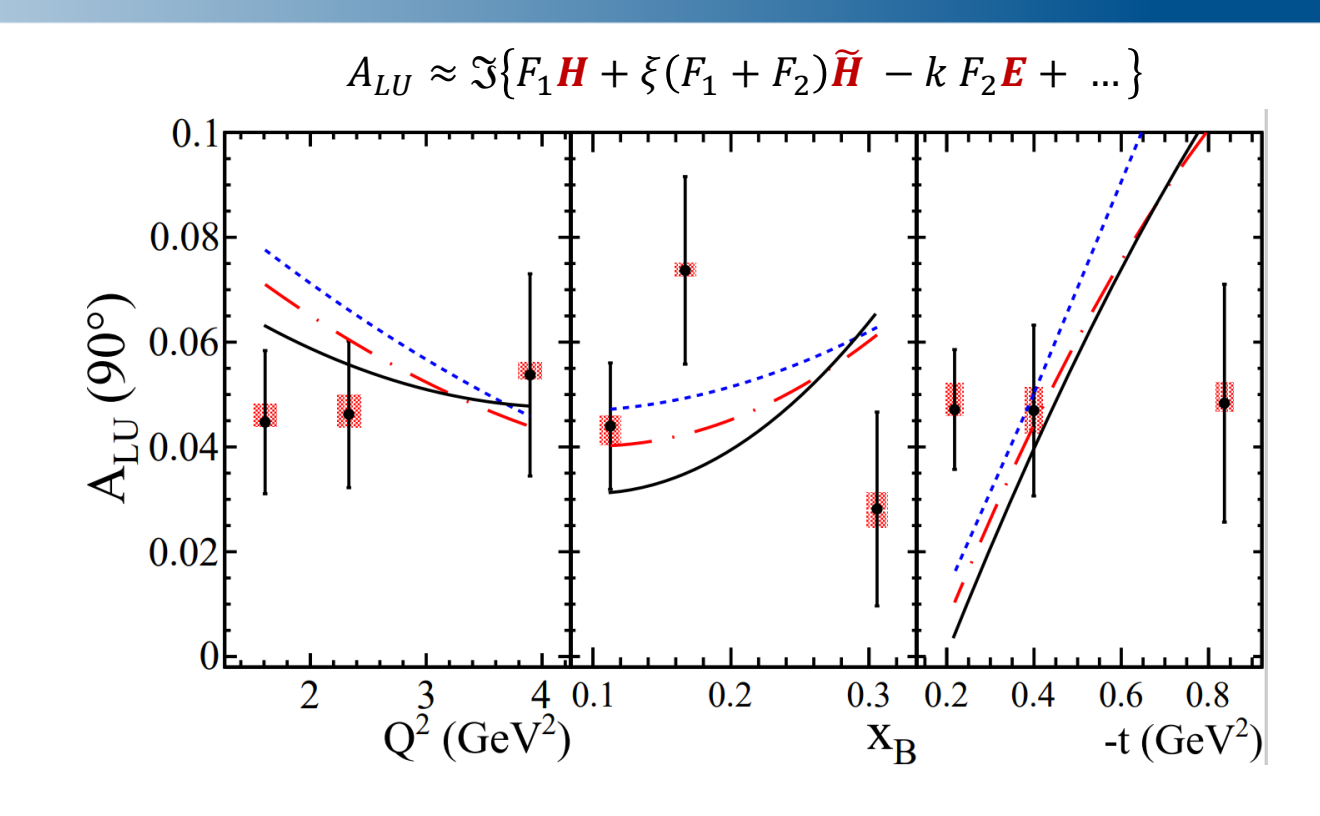


- Compared to the previous experiment, CLAS12 provides:
 - The possibility to scan the BSA of nDVCS on a wide phase space
 - The possibility to reach the high Q^2 high x_b region of the phase space
 - Exclusive measurement with the detection of the active neutron
- Hall A @ JLAB: one measured kinematical point at $Q^2=1.9 \text{ GeV}^2$ and $x_g=0.36$



CLAS12: nDVCS with an unpolarized deuterium target

- Observation of positive BSA for nDVCS
- Systematic errors include:
 - Error due to beam polarization
 - Error due to selection cuts
 - Error due to residual proton contamination
 - Error due to merging of data sets with different energies
- Statistics is expected to double with remaining schedualed beam time and improvements with reconstruction software



VGG model predictions giving the smallest χ^2

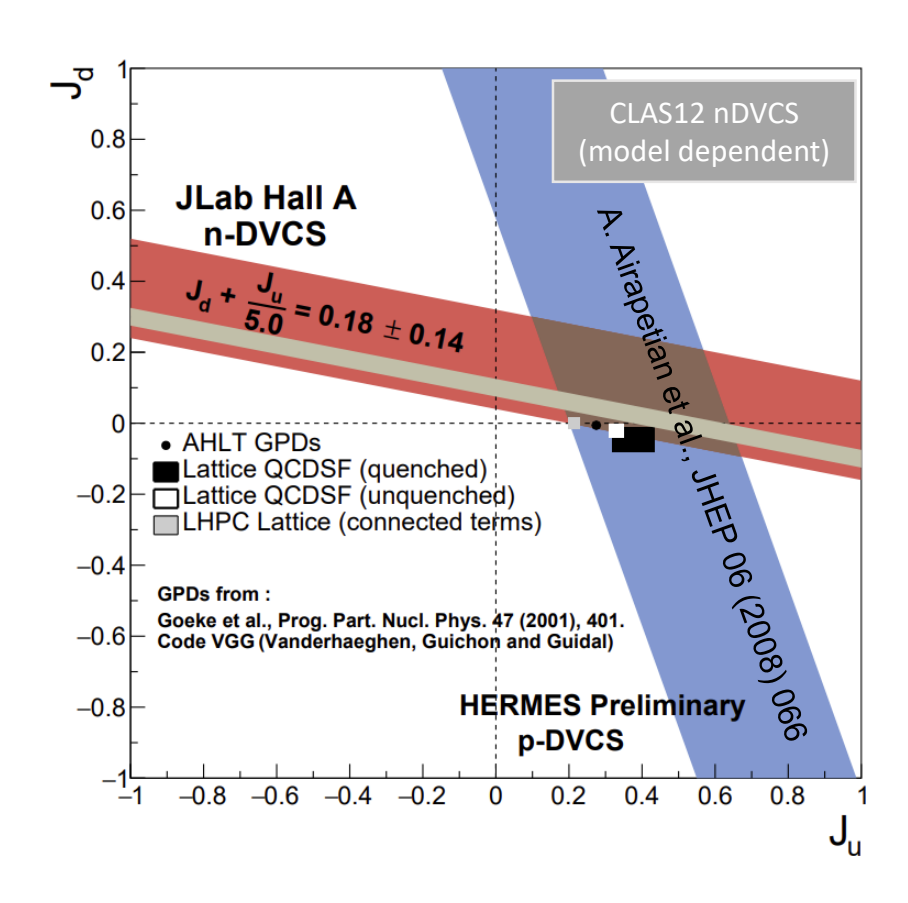
$$J_u = 0.35$$
 $J_d = 0.05$
 $J_u = -0.2$ $J_d = 0.15$
 $J_u = -0.45$ $J_d = 0.2$

M. Vanderhaeghen, P.A.M. Guichon, and M. Guidal, PRD 60, 094017 (1999)



Impact of nDVCS BSA data from CLAS12

- Model-dependant extraction of J_u and J_d
 - Use VGG model (PRD 60, 094017 (1999)) and generate a set of values for J_{II} and J_d
 - Look for the 1 standard deviation error ellipse: defined as $\chi^2 \chi^2_{min} \le 1$
- Compatible with limits set before by pioneering Hall A measurement
- Compatible with Lattice QCD predictions
- Shortcomings:
 - none of the considered sets of J_u and J_d reproduce correctly the distributions
 - VGG has problems in reproducing proton data
- Closest-to-truth model-dependent representation of data.

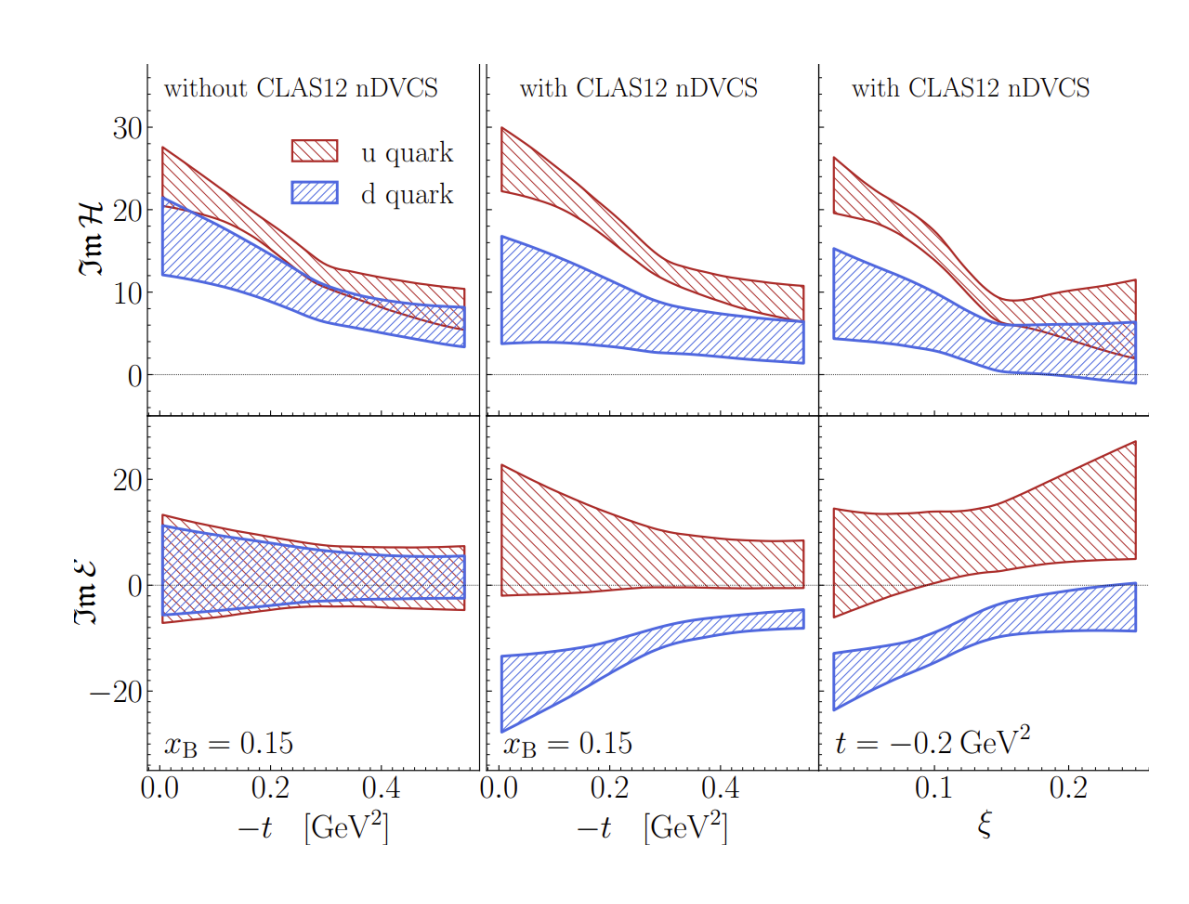




CFF extraction and flavor separation!

- Global fits of CFF using neural networks (model-independent)
 - K. Kumericki et al., JHEP 07, 073531 (2011);
 M. Cuic, K. Kumericki, et al., Phys. Rev. Lett. 533 125, 232005 (2020)).
- Data used:
 - CLAS6 and HERMES pDVCS observables
 - CLAS12 pDVCS BSA and nDVCS BSA
- Same extraction method applied to nDVCS Hall-A data, only separation for ImH

Clear quark-flavor separation of both ImH and ImE thanks to CLAS12 nDVCS data



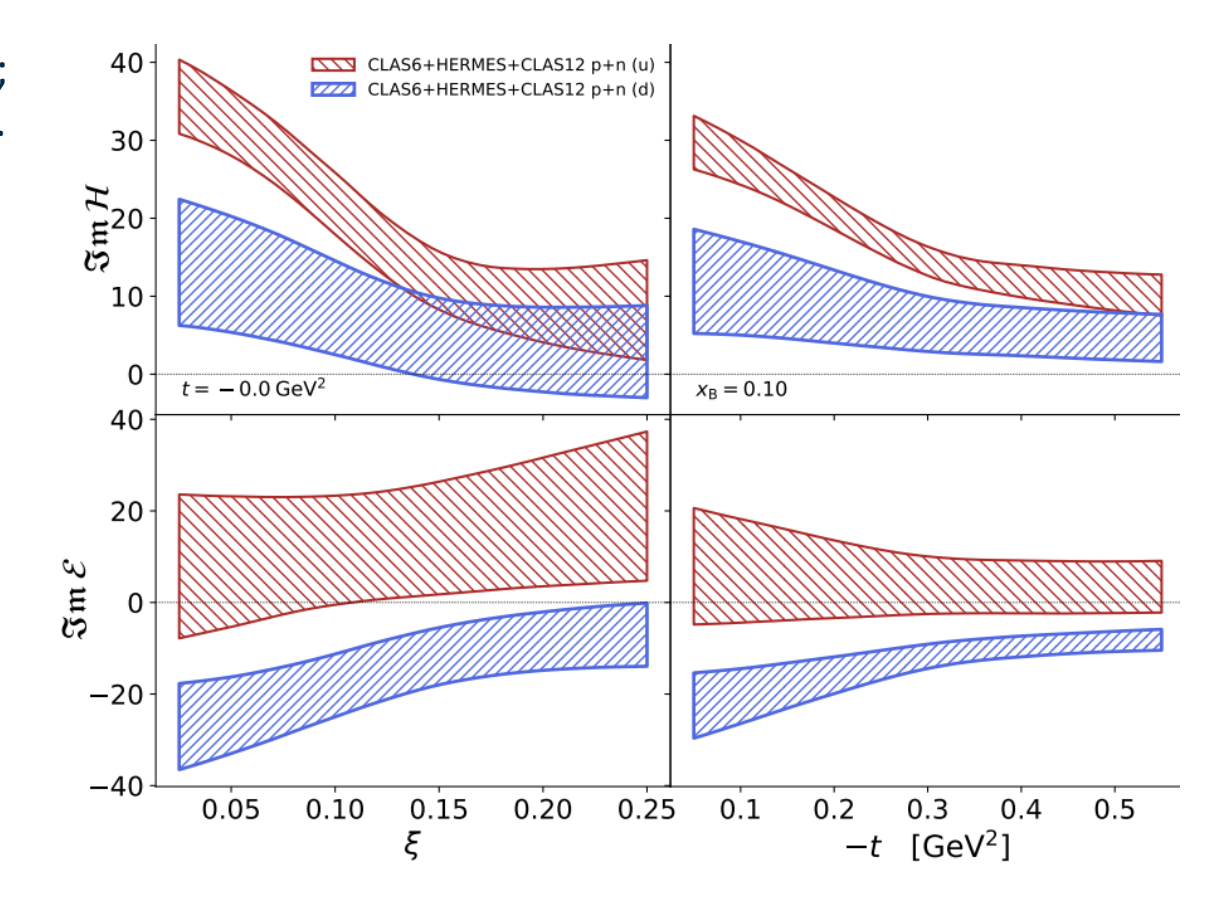


CFF extraction and flavor separation!

- Global fits of CFF using neural networks (model-independent)
 - K. Kumericki et al., JHEP 07, 073531 (2011);
 M. Cuic, K. Kumericki, et al., Phys. Rev. Lett. 533 125, 232005 (2020)).
- Data used:
 - CLAS6 and HERMES pDVCS observables
 - CLAS12 pDVCS BSA and nDVCS BSA
- Same extraction method applied to nDVCS Hall-A data, only separation for ImH

Clear quark-flavor separation of both ImH and ImE thanks to CLAS12 nDVCS data

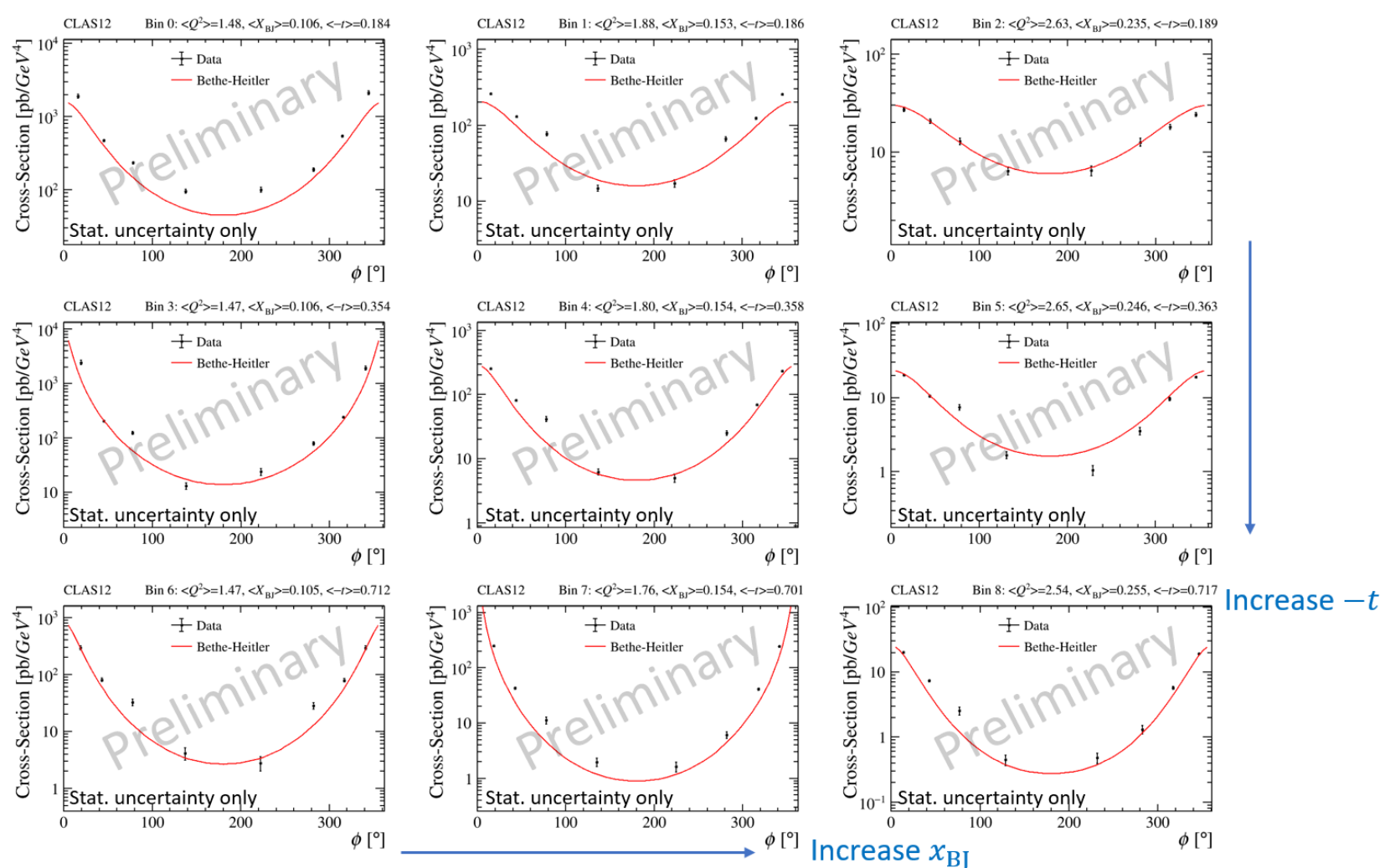
Results extrapolated to t=0 GeV²





Unpolarized nDVCS cross section

Credits: Li Xu



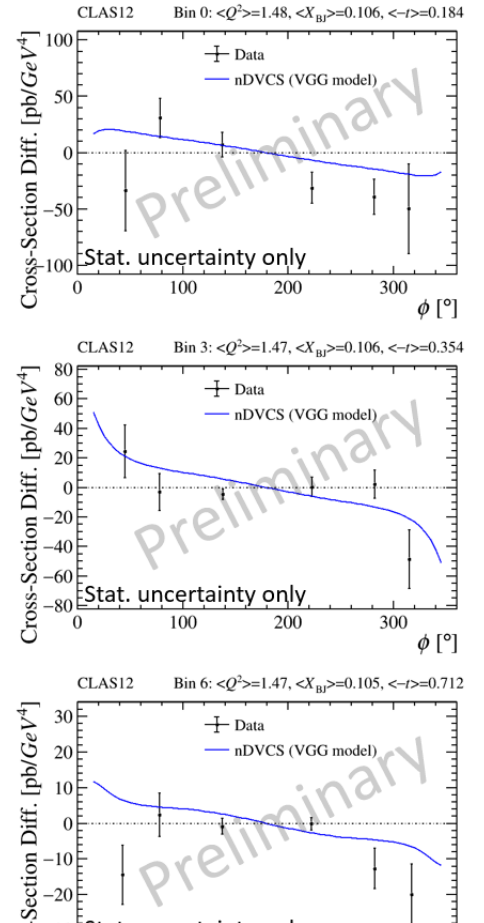
$$\sigma = \frac{N_{en \to en\gamma}}{L \cdot \varepsilon_{acc} \cdot V}$$

- Linked mainly to the real CFF of E
- Only the statistical uncertainty is presented
- The measured results are at the same level with the BH calculations



Polarized cross-section difference



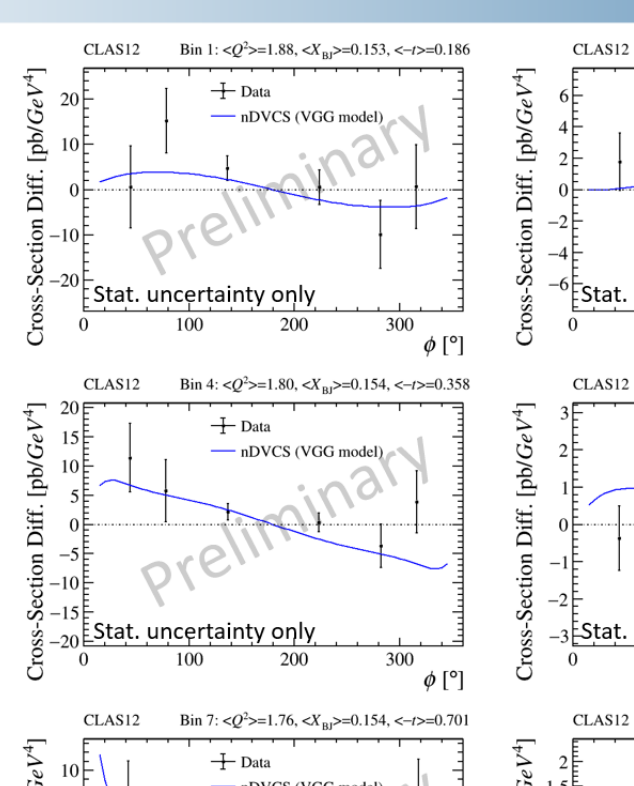


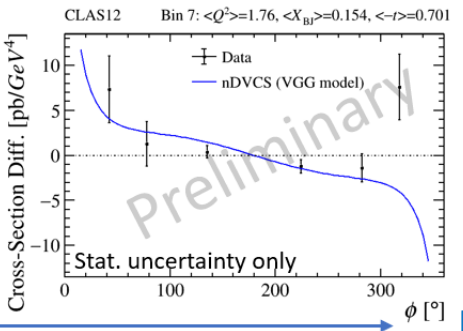
-30⊨Stat. uncertainty only

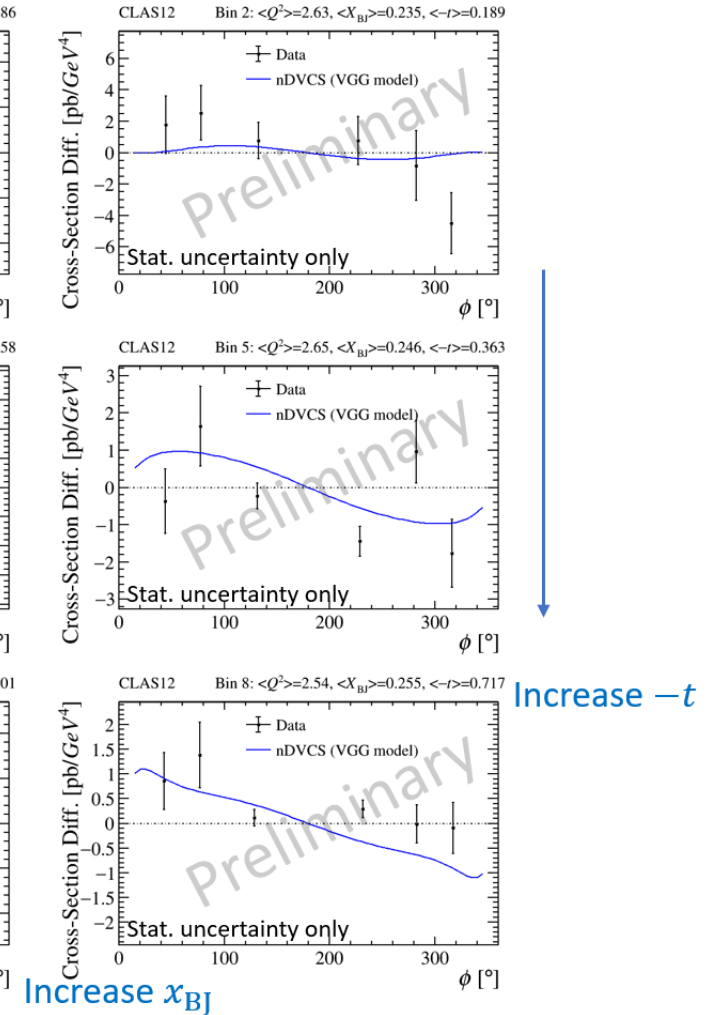
200

300

φ [°]







200

300 φ [°

$$\Delta \sigma = \frac{N_{+} - N_{-}}{L_{+(-)} \cdot P \cdot \varepsilon_{\rm acc} \cdot V}$$

- Linked to the imaginary CFF of E
- Only the statistical uncertainty is presented
- nDVCS predictions: VGG model with particular parameters $J_{u} = 0.3$ and $J_{d} = 0.1$
- The measured results are consistent with the predictions given the large statistical uncertainties

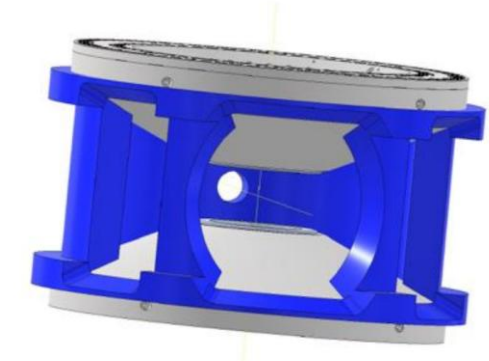


Coming on CLAS12: Transversely polarized target

Proposal: C12-24-RGH

- NH3: Viable solution to prioritize physics (2-3 yr)
 - Consolidated dynamically polarized technology
 - Designed based on already successful realizations
 - Hall-A G2p-Gep target (replica optimized for HTCC)
 - Hall-C E12-15-005 magnet (replica optimized for recoil detection)

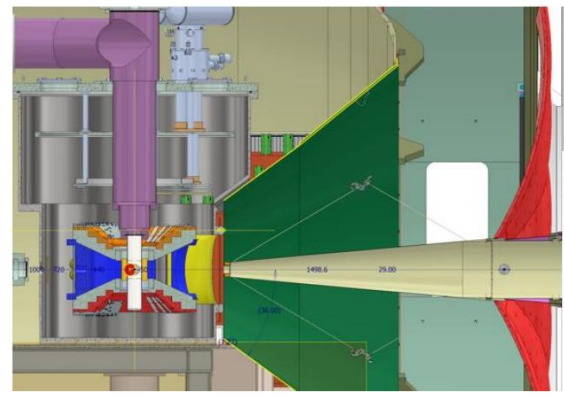




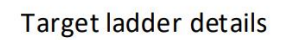
5T dipole acceptance:

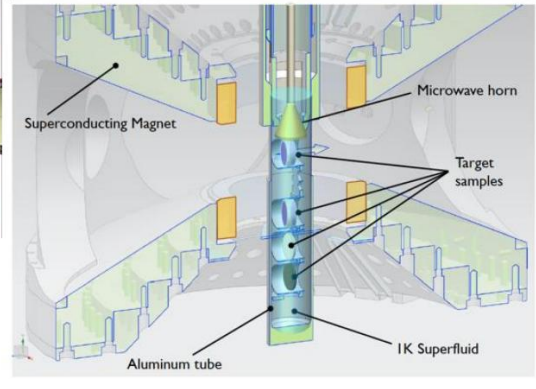
+ 25° vertical

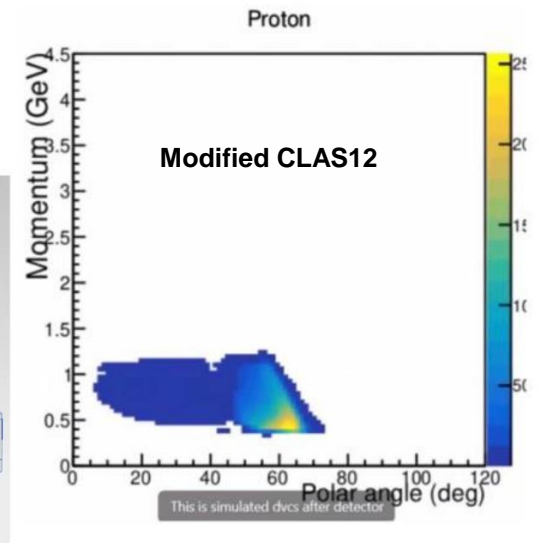
± 70° horizontal

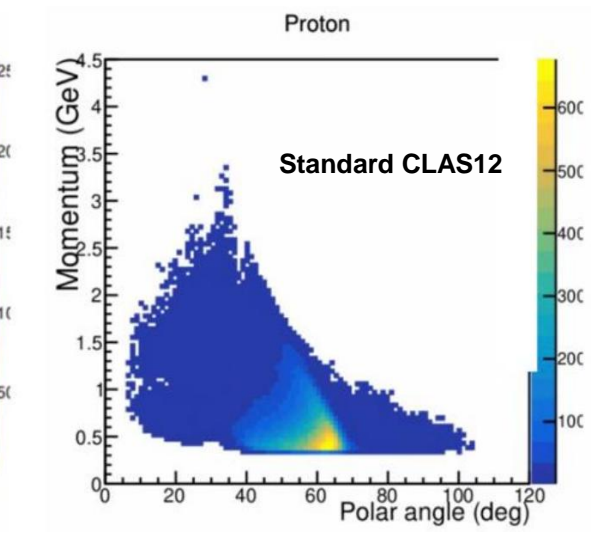


Target cryostat in front of CLAS12







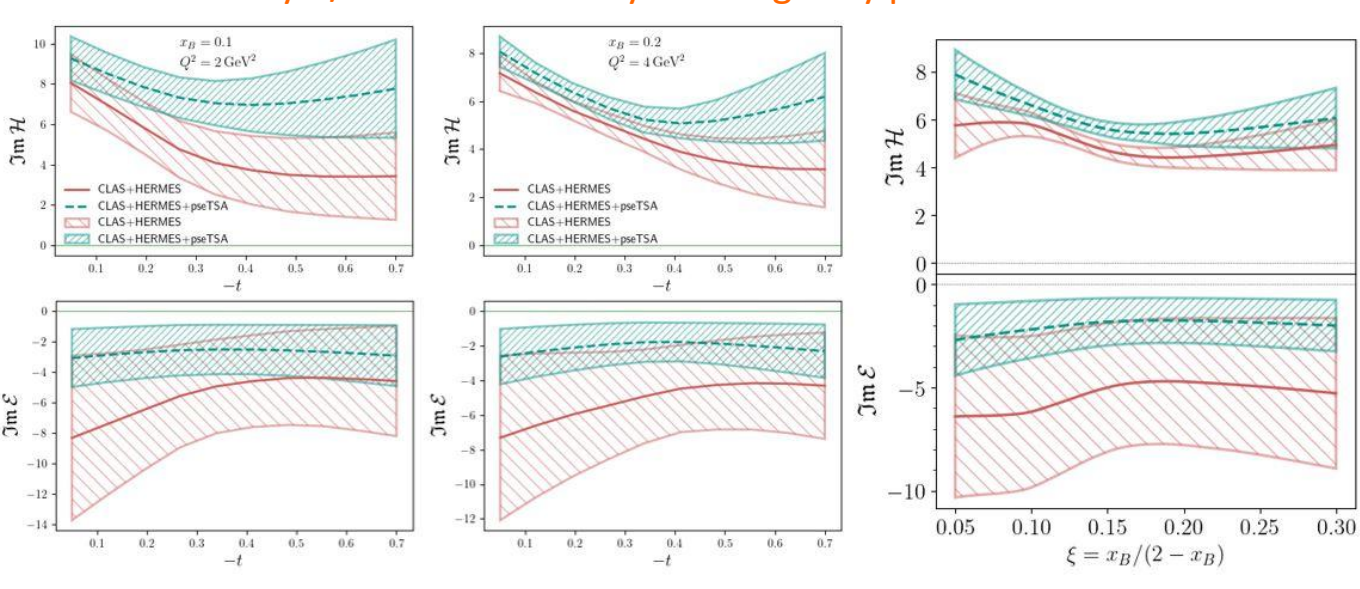


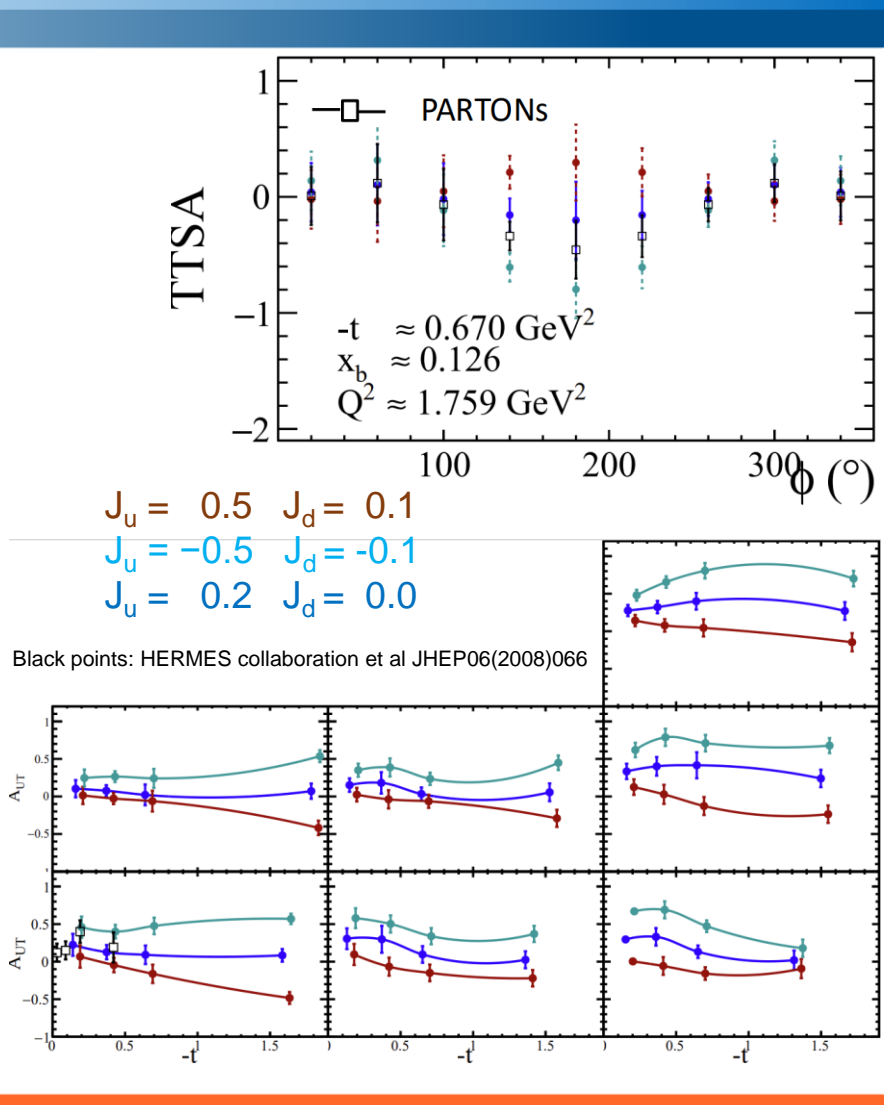


Coming on CLAS12: Transversely polarized target

Proposal: C12-24-RGH

- Unpolarized beam, transverse polarized target
 - $\Delta \sigma_{IJT} \sim \cos(\phi) \sin(\phi_s \phi) \Im\{k(F_2 \mathbf{H} F_1 \mathbf{E}) + ...\}$
- High impact expected on the extraction of the GPD E
 - 1 year to get unprecedented access to elusive quark angular momenta
 - Supersede the only other AUT measurement from HERMES collaboration
- Superior discrimination power between various OAM model hypotheses
- Reduce by 2/3 the uncertainty on imaginary part of CFF E





• Conservation of total angular momentum: off-diagonal TMDs vanish in absence of orbital angular momentum

$$\Delta \lambda = (\Lambda' - \Lambda) - (\lambda' - \lambda) \neq 0$$

 Λ : initial target light-front helicity Λ' : final target light-front helicity λ :initial parton light-front helicity λ' : final parton light-front helicity

• Some of these off-diagonal TMDs appear to be experimentally sizeable

Hermes Phys. Rev. Lett. 94 (2005) 012002 COMPASS Phys. Rev. Lett. 94 (2005) 202002 PHENIX Phys. Rev. D 82 (2010) 112008

• The quark Sivers TMD $f_{1T}^{\perp q}(x,k_{\perp}^2)$ and the quark GPD $E^q(x,\xi,t)$ could be related by a chromodynamic lensing mechanism

M. Burkardt Phys. Rev. D 66 (2002) 114005 and Nuclear Phys. A 735 (2004)

$$\int d^2k_\perp \, \frac{{\bf k}_\perp^2}{2{\sf M}^2} f_{1T}^{\perp q}(x,{\bf k}_\perp^2) \propto \int d^2b_\perp \, \overline{{\it T}}({\bf b}_\perp) ({\bf S}_T \times {\bf \partial}_{b_\perp})_z \, {\cal E}^q(x,{\bf b}_\perp^2)$$
 Lensing function

$$\mathcal{E}^{q}(x, \boldsymbol{b}_{\perp}^{2}) = \int \frac{d^{2} \Delta_{\perp}}{(2\pi)^{2}} e^{-i\boldsymbol{b}_{\perp} \cdot \boldsymbol{\Delta}_{\perp}} E^{q}(x, 0, -\boldsymbol{\Delta}_{\perp}^{2})$$

• The Sivers function could then be used to constrain the GPD E^q and hence the kinetic OAM via the Ji sum rule.

 Performed previously by Bacchetta and Radici in Phys. Rev. Lett. 107, 212001 using proton data from HERMES, neutron and deuteron data from Jlab hall A and COMPAS



More on DVCS at CLAS12

- The second half of Run Group B will run providing extra statistics.
- The combination of all neutron and proton DVCS data will allow quark-flavor separation of all CFFs in the valence region
- The Ji's sum rule is the ultimate, ambitious goal of this program



Conclusions

- The beam -spin asymmetry for nDVCS is a precious tool to constrain the GPD E and for quark -flavor separation of GPDs
- CLAS12 measured the BSA for nDVCS with detected neutron for the first time
- The first ~43% of the experiment ran in 2019 -2020 at llab
- A small but clear BSA was extracted
- Comparison with a model allows to put modeldependent constraints on J_d
- The data, together with the proton DVCS data, allow the quark -flavor separation of ImH and ImE

PHYSICAL REVIEW LETTERS 133, 211903 (2024)

First Measurement of Deeply Virtual Compton Scattering on the Neutron with Detection of the Active Neutron

A. Hobart[©], ¹ S. Niccolai, ¹ M. Čuić, ² K. Kumerički, ² P. Achenbach, ³ J. S. Alvarado, ¹ W. R. Armstrong, ⁴ H. Atac, ⁵ H. Avakian, ³ L. Baashen, ^{6*} N. A. Baltzell, ³ L. Barion, ⁷ M. Bashkanov, ⁸ M. Battaglieri, ^{39,7†} B. Benkel, ¹⁰ F. Benmokhtar, ¹¹ A. Bianconi, ^{12,13} A. S. Biselli, ¹⁴ S. Boiarinov, ³ M. Bondi, ¹⁵ W. A. Booth, ⁸ F. Bossù, ¹⁶ K.-Th. Brinkmann, ¹⁷ W. J. Briscoe, ¹⁸ W. K. Brooks, ¹⁹ S. Bueltmann, ²⁰ V. D. Burkert, ³ T. Cao, ³ R. Capobianco, ²¹ D. S. Carman, ³ P. Chatagnon, ^{3,1} G. Ciullo, ^{7,22} P. L. Cole, ²³ M. Contalbrigo, ⁷ A. D'Angelo, ^{10,24} N. Dashyan, ²⁵ R. De Vita, ^{9,4} M. Defurne, ¹⁶ A. Deur, ³ S. Diehl, ^{17,21} C. Dilks, ^{3,26} C. Djalali, ²⁷ R. Dupre, ¹ H. Egiyan, ³ A. El Alaoui, ¹⁹ L. El Fassi, ²⁸ L. Elouadrhiri, ³ S. Fegan, ⁸ A. Filippi, ²⁹ C. Fogler, ²⁰ K. Gates, ³⁰ G. Gavalian, ^{3,31} G. P. Gilfoyle, ³² D. Glazier, ³⁰ R. W. Gothe, ³³ Y. Gotra, ³ M. Guidal, ¹ K. Hafidi, ⁴ H. Hakobyan, ¹⁹ M. Hattawy, ²⁰ F. Hauenstein, ^{3,20} D. Heddle, ^{34,3} M. Holtrop, ³¹ Y. Ilieva, ^{33,18} D. G. Ireland, ³⁰ E. L. Isupov, ³⁵ H. Jiang, ³⁰ H. S. Jo, ³⁶ K. Joo, ²¹ T. Kageya, ³ A. Kim, ²¹ W. Kim, ³⁶ V. Klimenko, ²¹ A. Kripko, ¹⁷ V. Kubarovsky, ^{3,37} S. E. Kuhn, ²⁰ L. Lanza, ^{10,24} M. Leali, ^{12,13} S. Lee, ^{4,38} P. Lenisa, ^{7,22} X. Li, ³⁸ I. J. D. MacGregor, ³⁰ D. Marchand, ¹ V. Mascagna, ^{12,39,13} M. Maynes, ²⁸ B. McKinnon, ³⁰ Z. E. Meziani, ⁴ S. Migliorati, ^{12,13} R. G. Milner, ³⁸ T. Mineeva, ¹⁹ M. Mirazita, ⁴⁰ V. Mokeev, ^{3,55} C. Muñoz Camacho, ¹ P. Nadel-Turonski, ³ P. Naidoo, ³⁰ K. Neupane, ³³ G. Niculescu, ⁴¹ M. Osipenko, ⁹ P. Pandey, ³⁸ M. Paolone, ^{42,5} L. L. Pappalardo, ^{7,22} R. Paremuzyan, ^{3,31} E. Pasyuk, ³ S. J. Paul, ⁴³ W. Phelps, ^{34,3} N. Pilleux, ¹ M. Pokhrel, ²⁰ S. Polcher Rafael, ¹⁶ J. Poudel, ³ J. W. Price, ⁴⁴ Y. Prok, ²⁰ T. Reed, ⁶ J. Richards, ²¹ M. Ripani, ¹ J. Ritman, ^{45,46} P. Rossi

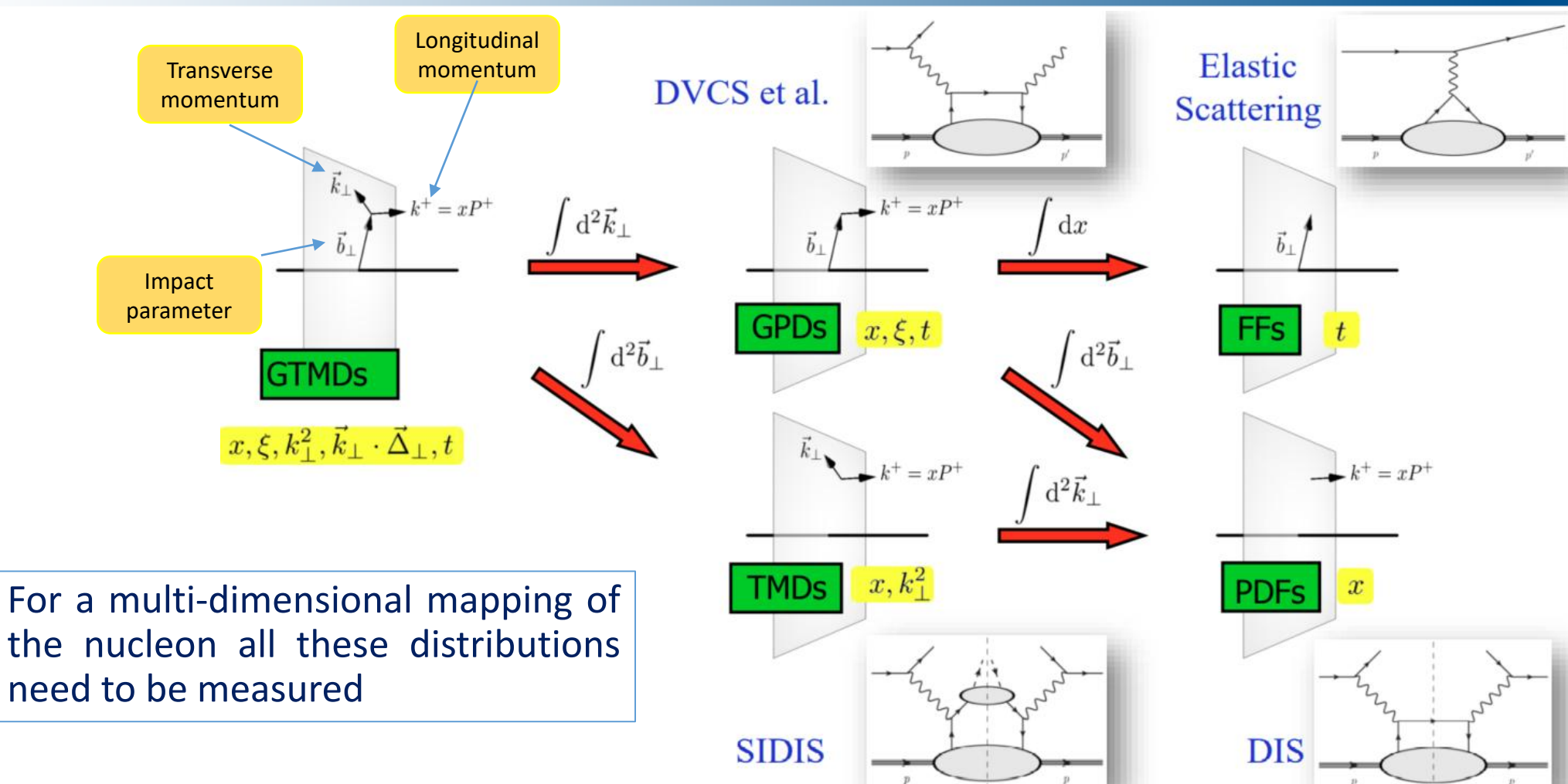
(CLAS Collaboration)



Backups



Multi-dimensional mapping of nucleon structure



M. A. HOBALLAH EINN 2025



Summary

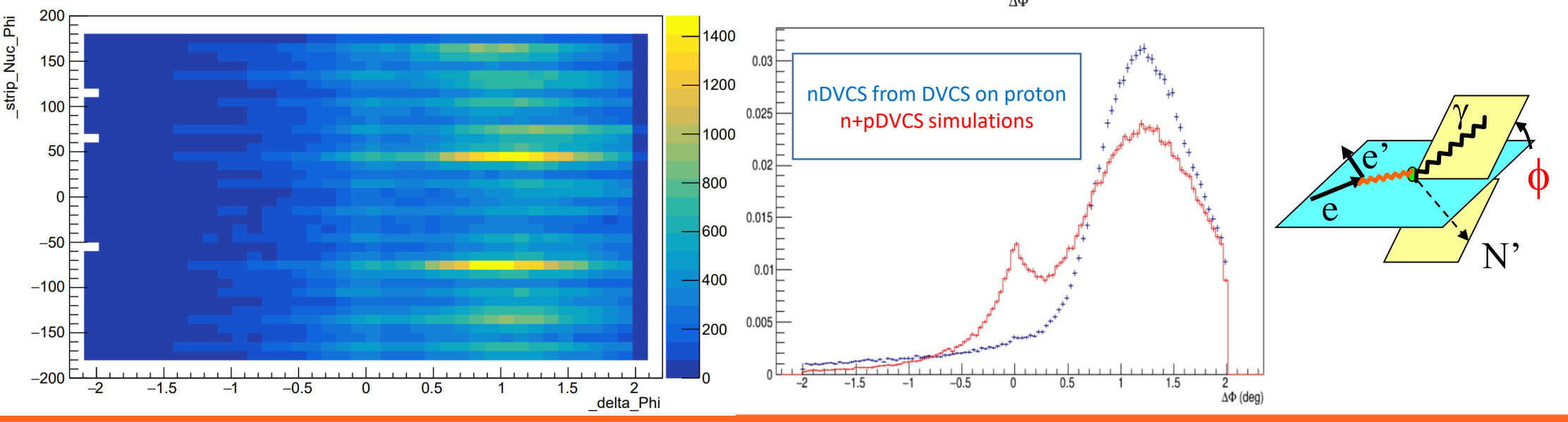
- GPDs are powerful tool to explore the structure of the nucleons and nuclei
 - Nucleon tomography, quark angular momentum, distribution of forces in the nucleon
- Exclusive reactions can provide important information on nucleon structure
 - DVCS via the extraction of GPDs
- CLAS12 offers a wide kinematical reach over which the GPDs dependence on different kinematical variables can be scanned
 - Data to add constraints on GPDs in unexplored regions of the phase space
 - Possibilities to measure new observables using different experimental configurations
 - Flavor separation of GPDs
- Promising results from incoherent DVCS on deuteron (n and p channels) from CLAS12 data
 - First BSA measurement from neutron-DVCS with tagged neutron
 - First measurement of BSA for proton-DVCS with deuterium target
 - To be compared to free-proton DVCS BSA measured by CLAS12

G. Christiaens, M. Defurne, D. Sokhan V. Ziegler et al., Phys. Rev. Lett. 130 (21) 211902 (2023)



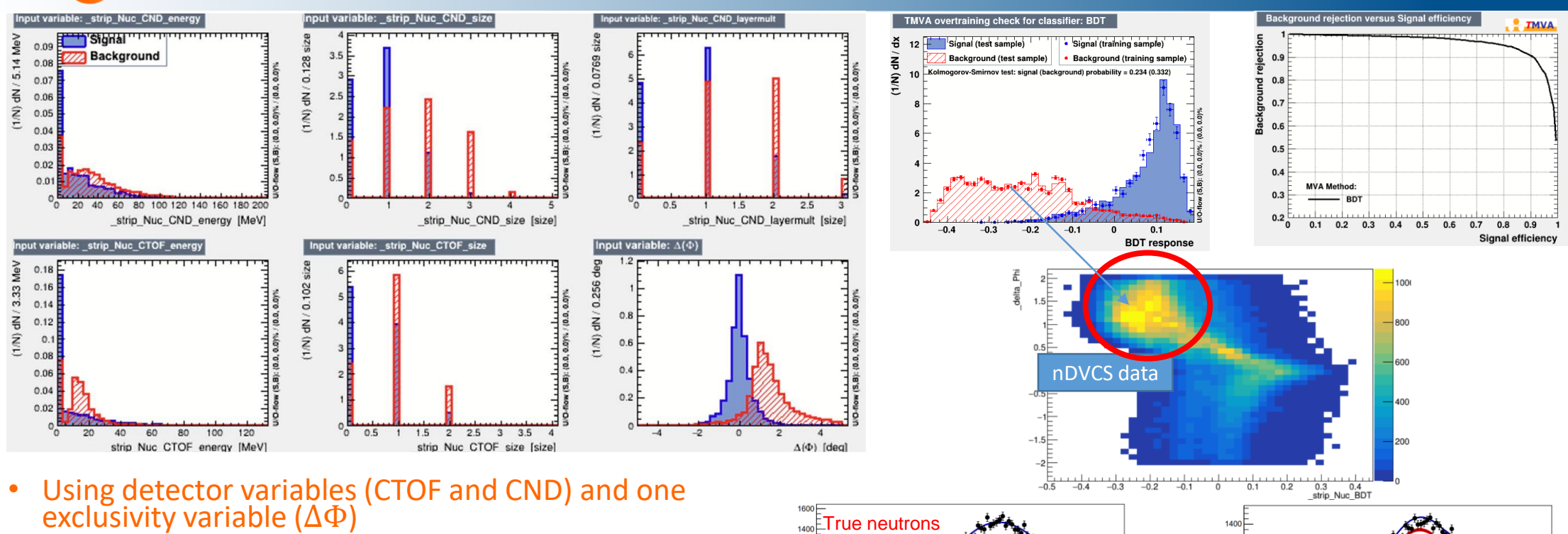
Improving the neutron selection with ML techniques

- The tracking of the CVT is neither 100% efficient nor uniform
- In the dead regions of the CVT protons have no associated track and thus can be misidentified as neutrons
- Protons roughly account for more than >40% contamination in the "nDVCS" signal sample Current approach, based on Machine Learning & Multi-Variate Algorithms:
 - We reconstruct nDVCS from DVCS experiment on proton requiring neutron PID : selected neutron are misidentified protons
 - We use this sample to determine the characteristics of fake neutrons in low- and high-level reconstructed variables
 - Based on those characteristics we subtract the fake neutrons contamination from nDVCS
 - As a « signal » sample in the training of the ML we use $ep \to en\pi^+$ events from DVCS experiment on proton

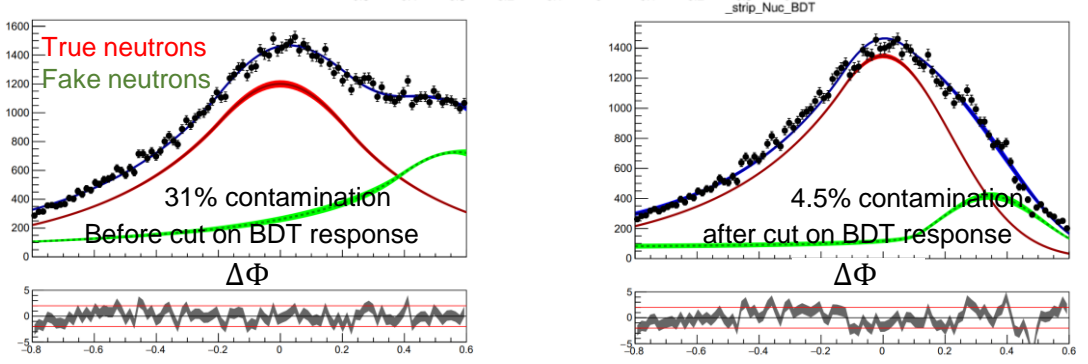




Improving the neutron selection with ML techniques



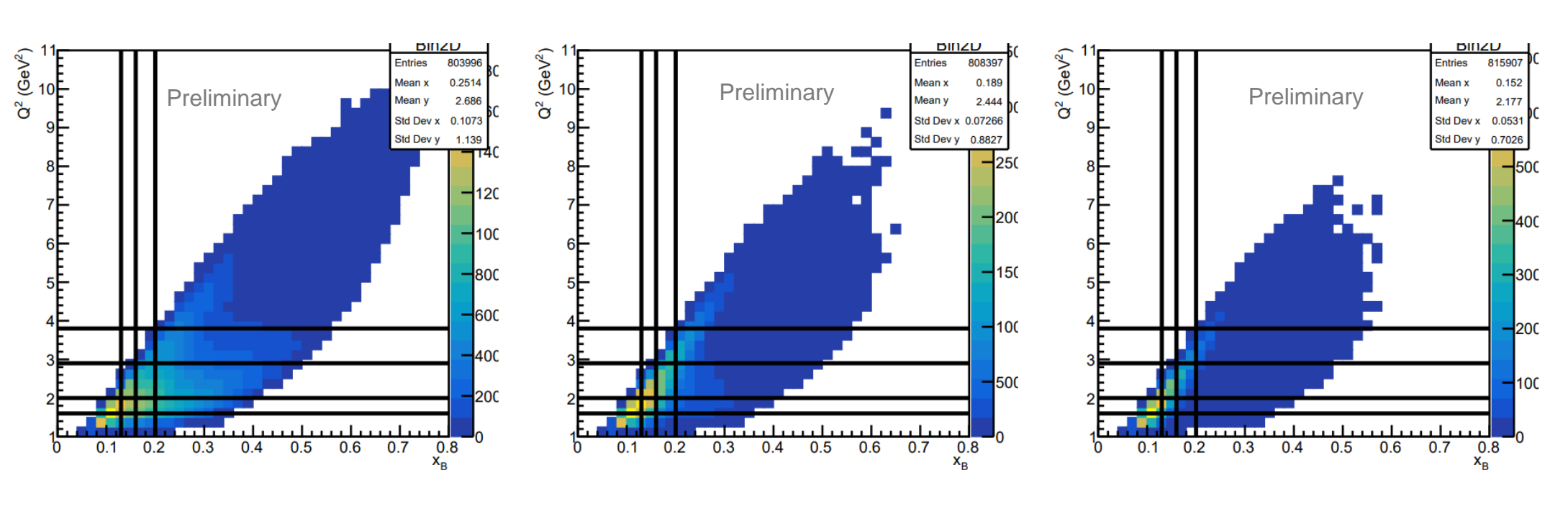
- Directly trained on data
- Better optimization of signal to background ratio than straight cuts
- Few percent irreducible contamination corrected for in the final BSA





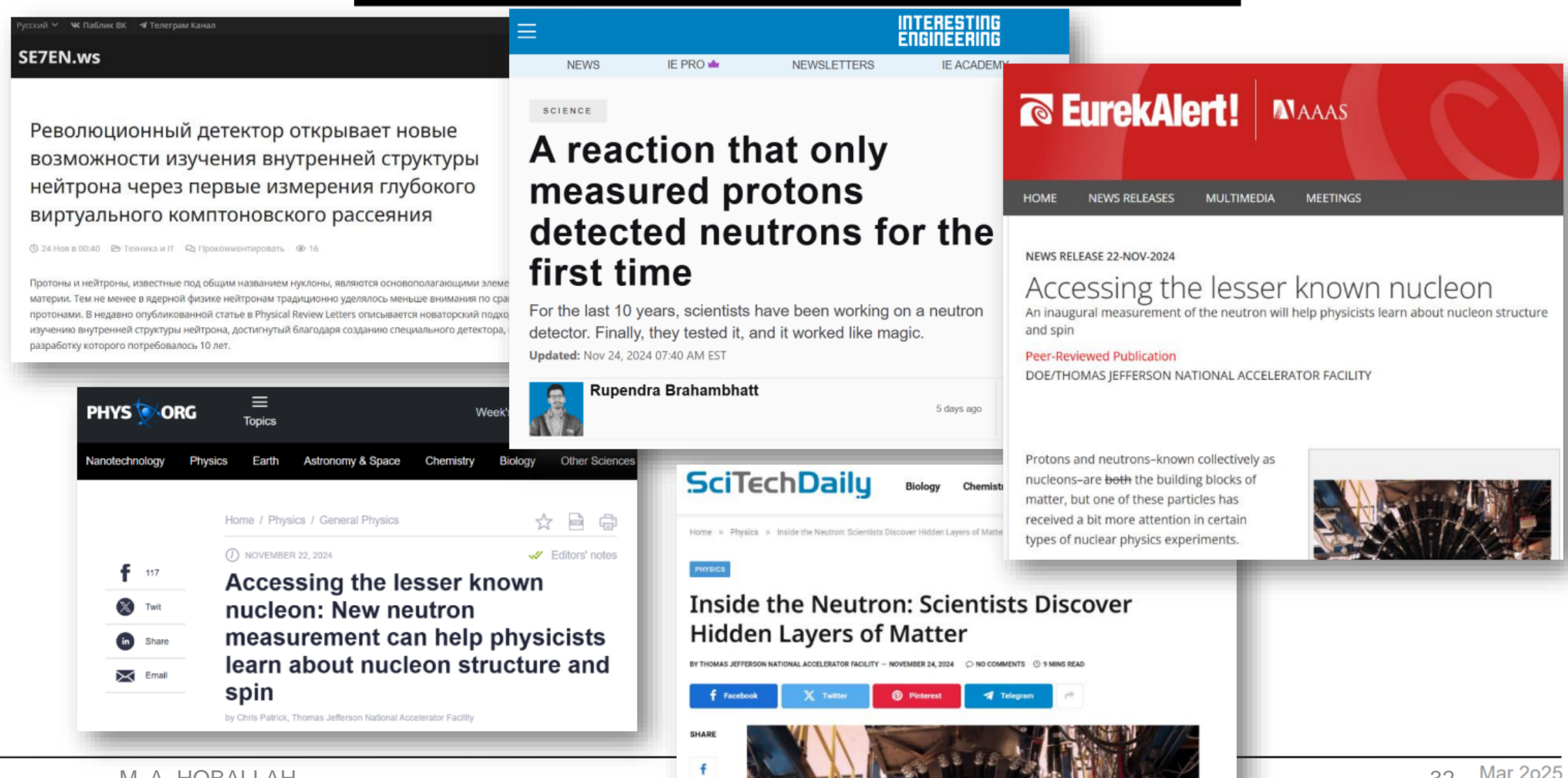
CLAS12: pDVCS with an unpolarized deuterium target

First-time measurement of incoherent pDVCS on deuteron



- Complementary to previous experiment on proton target:
 - Quantify medium effects on GPDs

Media Coverage of News Release Nov 2024



Foreign Media Coverage of News Release



Visão inédita dos nêutrons ajuda a entender ainda mais a composição da matéria

Pesquisa revela detalhes sobre a distribuição dos quarks nos nêutrons

Ronnie Mancuzo | ① 07/12/2024 19h05

Home » Los científicos descubren capas ocultas de materia

Tecnología

LOS CIENTÍFICOS DESCUBREN CAPAS OCULTAS DE MATERIA

24/11/2024

daily geek show



Des scientifiques dévoilent la structure interne d'un neutron avec une précision effarante

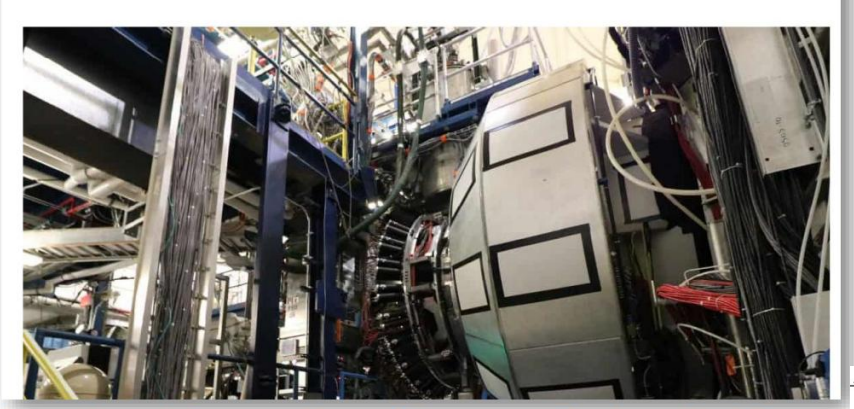
Une étude qui a demandé plus de dix ans d'efforts

Follow-up in *Physics News* 17 Dec 2024

physicsworld

PARTICLE AND NUCLEAR RESEARCH UPDATE

Inner workings of the neutron illuminated by Jefferson Lab experiment



https://physicsworld.com/a/inner-workings-of-the-neutron-illuminated-by-jefferson-l

Glimpse of The Neutron (Al Generated?)



Huge Experiment Gives First Glimpse of The Internal Structure of a Neutron

PHYSICS 07 December 2024 By MIKE MCRAE



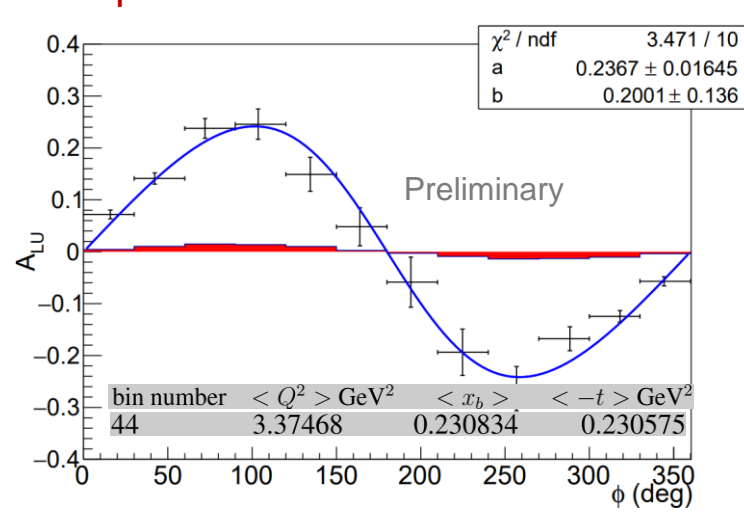
M. A. HOBALLAH

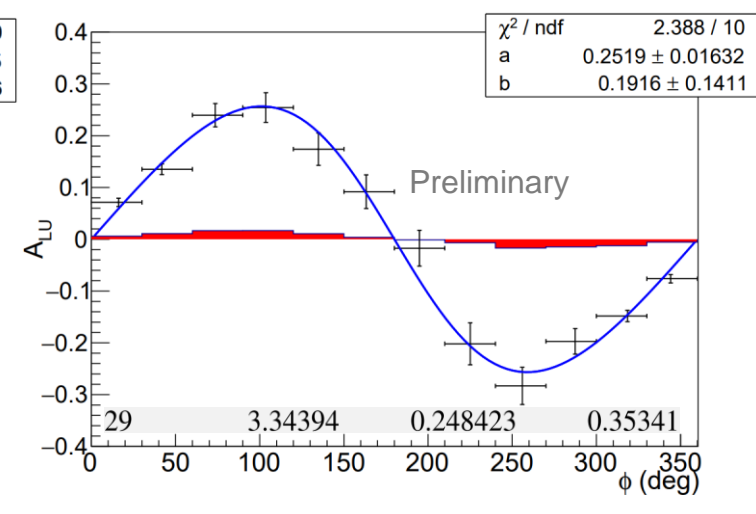
- 34

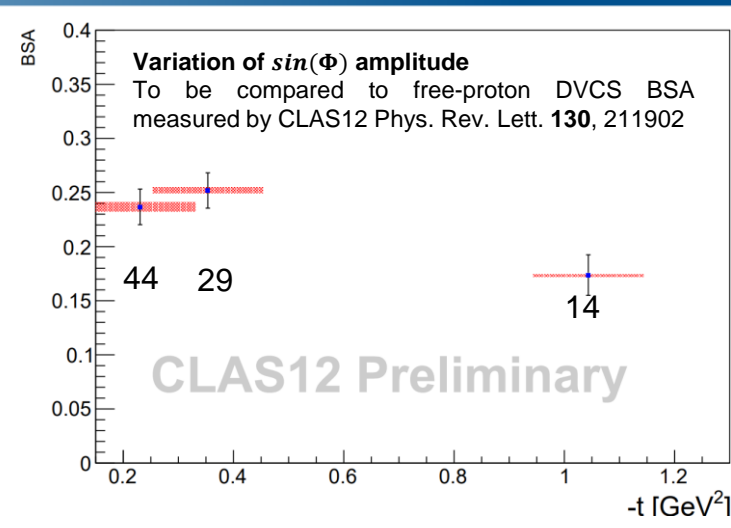


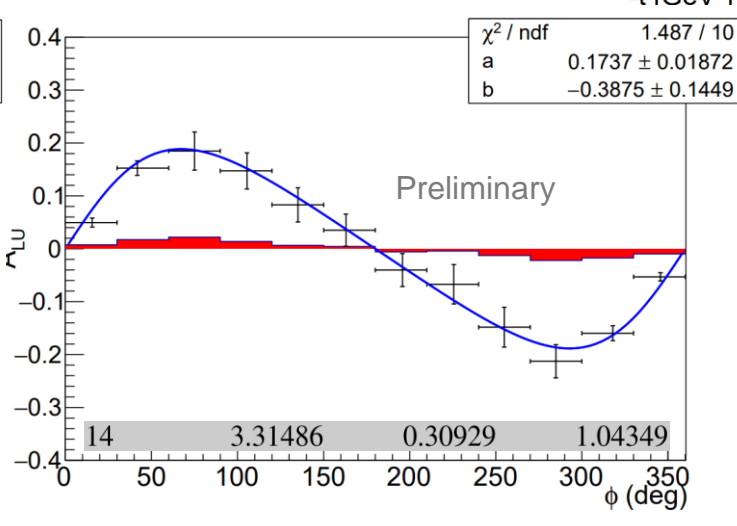
CLAS12: pDVCS with an unpolarized deuterium target

- First-time measurement of incoherent pDVCS on deuteron
 - Quantify medium effects on GPDs
- Systematic errors include:
 - Error due to beam polarization
 - Error due to selection cuts
 - Error due to merging of data sets with different energies
- Statistics is expected to triple with remaining schedualed beam time and improvements with reconstruction software











CLAS12: pDVCS with an unpolarized deuterium target

